Published for SISSA by Springer

Received: *May 20, 2026*
Accepted: *September 4, 2026*
Published: *October 19, 2026*

Search for soft unclustered energy patterns containing muons in the final state in pp collisions at $\sqrt{s} = 13$ TeV with the ATLAS detector



The ATLAS collaboration

Full author list at the end of the paper

E-mail: atlas.publications@cern.ch

Abstract: Soft unclustered energy patterns (SUEPs) refer to high-multiplicity, isotropic distributions of low-momentum particles that could arise in strongly-coupled hidden sector theories. A search for SUEPs whose decay products contain muons in the final state is presented using 140 fb^{-1} of proton–proton collision data at $\sqrt{s} = 13$ TeV collected by the ATLAS detector at the Large Hadron Collider during 2015–2018. The analysis targets SUEP signatures via gluon–gluon fusion production of a scalar mediator in Hidden Valley scenarios. No significant excess over the Standard Model expectation is observed. Exclusion limits are set on the product of the mediator production cross section and the branching fraction for its decay into a SUEP, down to 0.05 fb for a mediator mass of $m_S = 750$ GeV, 0.4 fb for $m_S = 400$ GeV, and 70 fb for $m_S = 125$ GeV; the last value, when identifying the mediator with the Standard Model Higgs boson, translates to an upper limit on the branching fraction of around 0.2%.

Keywords: Beyond Standard Model, Exotics, Hadron-Hadron Scattering, Dark Matter

ArXiv ePrint: 2605.20015

Open Access, Copyright CERN,
for the benefit of the ATLAS Collaboration.
Article funded by SCOAP^3.

https://doi.org/10.1007/JHEP10(2026)206

Contents

1 Introduction **1**

2 ATLAS detector **3**

3 Data and simulated event samples **4**

4 Event reconstruction **6**
4.1 Sphericity 8
4.2 Track multiplicity 9

5 Event selection and background estimation **11**

6 Systematic uncertainties **14**

7 Statistical analysis and results **16**

8 Conclusion **21**

The ATLAS collaboration **28**

1 Introduction

Hidden Valley (HV) models [1, 2] provide a well-motivated extension of the Standard Model (SM) in which a hidden sector, neutral under SM gauge interactions, is connected to the SM visible sector through weak, so-called *portal* interactions. Such scenarios arise naturally in solutions to the hierarchy problem, which often introduce additional sectors with suppressed couplings to the SM [3]. Strongly interacting hidden sectors are further motivated by the possibility that dark matter is composed of bound states of a QCD-like hidden force [4, 5], or that it resides in a dark sector with sizable self-interactions, as suggested by small-scale structure anomalies in galaxies and their clusters [6–8].

At the Large Hadron Collider (LHC), a range of searches has targeted these scenarios in regimes where the hidden sector undergoes a shower analogous to a QCD parton shower, giving rise to jet-like signatures once the hidden-sector particles decay to visible SM particles. These include searches for so-called semi-visible jets [9–11] and emerging jets [12, 13], which exploit the resulting exotic jet topologies to distinguish such events from SM backgrounds.

However, if the hidden-sector force remains strongly coupled well above its hadronization scale, corresponding to a quasi-conformal coupling regime, its radiation pattern can differ qualitatively from that of QCD. In particular, emissions need not be dominated by soft and collinear splittings, and the resulting shower may instead populate phase space more uniformly [14–17]. For models in which the available energy is distributed among many particles, this results in a characteristic collider signature known as a *Soft Unclustered Energy Pattern* (SUEP), consisting of a high multiplicity of low-momentum particles, distributed approximately isotropically in the center-of-mass frame [14, 18]. Figure 1 shows a repre-

JHEP10(2026)206

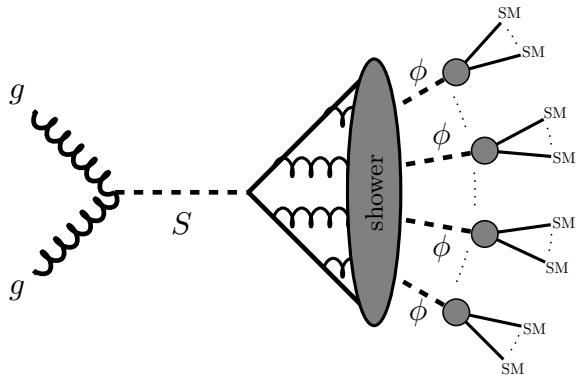


Figure 1. Representative diagram of gluon-fusion production of a scalar mediator S, followed by showering in the dark sector and the production of a high-multiplicity final state of light dark (pseudo-)scalars (ϕ). The ϕ particles subsequently decay promptly to SM particles through their coupling to dark photons, which mix kinetically with the SM photon. The figure is taken from ref. [18].

sentative signal diagram. The absence of hard or collimated objects makes such signatures challenging both to trigger on and to reconstruct. Exploring such unconventional and experimentally challenging signatures is essential to ensure sensitivity to a broad range of possible extensions of the SM.

Both the existing searches for SUEP signatures performed by the CMS Collaboration [19, 20] and the analysis presented here are based on the theoretical framework proposed in ref. [18]. In this framework, the hidden sector is accessed through a scalar portal, which may be the SM Higgs boson or a heavier scalar particle. Within the dark sector, particles undergo showering and subsequently hadronize into a large number of dark mesons ϕ, which are assumed for simplicity to consist of a single particle species. A wide range of values for the dark-meson mass m_ϕ is theoretically motivated. Generally, values of order 1–10 GeV are well suited for SUEP scenarios, as they allow for a rich set of decay channels to SM particles while still producing the high-multiplicity, soft final states characteristic of this signature, which are not efficiently targeted by conventional searches. The momenta of the dark mesons are expected to follow an approximately thermal distribution [21] and are modeled using a Maxwell–Boltzmann spectrum parameterized by a Hagedorn temperature T [22], which sets the characteristic momentum scale of the hadronizing hidden sector and is expected to be of the same order as m_ϕ. The dark mesons are assumed to decay promptly into pairs of dark photons (A'), which subsequently decay promptly into charged SM particles via kinetic mixing with the SM photon [23]. While other decay modes of dark mesons to SM particles are possible [24], this choice provides a convenient and realistic framework to realize a wide range of final-state particle compositions. For a given dark-photon mass, the branching fractions to SM particles are fixed, leading to specific mixtures of electrons, muons, and hadrons in the final state. For dark-photon masses of order 1 GeV, the dominant decay modes are $A' \to e^+e^-$, $A' \to \mu^+\mu^-$, and $A' \to \pi^+\pi^-$.

A previous search for SUEP signatures by the CMS Collaboration [19] targeted gluon–gluon fusion production of the mediator and relied on high-transverse-momentum initial-state radiation to trigger events via large energy deposits in the calorimeters. While this approach

JHEP10(2026)206

provided sensitivity over a broad range of T and m_ϕ, it was primarily sensitive to scenarios with large mediator masses. Subsequent searches targeting associated production of the Higgs boson with a vector boson [20] complemented this result. However, the requirement of very high particle multiplicities to suppress background limited the sensitivity to scenarios with low m_ϕ and T.

The search presented here complements these approaches by targeting final states with a high multiplicity of prompt muons, which are expected for a broad range of dark-photon masses $m_{A'}$. This strategy provides strong background rejection while maintaining sensitivity to scenarios with moderate particle multiplicities, thereby extending the coverage of the SUEP parameter space well beyond that of previous searches.

Events are selected using multi-muon triggers and target prompt final states with a high multiplicity of muons. They are further characterized by relatively low average muon transverse momentum, large charged-particle track multiplicity associated with the primary interaction, and isotropic spatial distribution of the muons. The signal region is defined to be sensitive to a broad range of charged-particle multiplicities and to preferentially select events in which muons are distributed more isotropically than in the dominant background from QCD multijet production, where muons are produced mainly in heavy-flavor decays, and which is estimated using a data-driven method.

2 ATLAS detector

The ATLAS detector [25] at the LHC covers nearly the entire solid angle around the collision point.[1] It consists of an inner tracking detector surrounded by a thin superconducting solenoid, electromagnetic and hadronic calorimeters, and a muon spectrometer incorporating three large superconducting air-core toroidal magnets.

The inner-detector system (ID) is immersed in a 2 T axial magnetic field and provides charged-particle tracking in the range $|\eta| < 2.5$. The high-granularity silicon pixel detector covers the vertex region and typically provides four measurements per track, the first hit generally being in the insertable B-layer (IBL) installed before Run 2 [26, 27]. It is followed by the SemiConductor Tracker (SCT), which usually provides eight measurements per track. These silicon detectors are complemented by the transition radiation tracker (TRT), which enables radially extended track reconstruction up to $|\eta| = 2.0$. The TRT also provides electron identification information based on the fraction of hits (typically 30 in total) above a higher energy-deposit threshold corresponding to transition radiation.

The calorimeter system covers the pseudorapidity range $|\eta| < 4.9$. Within the region $|\eta| < 3.2$, electromagnetic calorimetry is provided by barrel and endcap high-granularity lead/liquid-argon (LAr) calorimeters, with an additional thin LAr presampler covering $|\eta| < 1.8$ to correct for energy loss in material upstream of the calorimeters. Hadronic

[1] ATLAS uses a right-handed coordinate system with its origin at the nominal interaction point (IP) in the centre of the detector and the z-axis along the beam pipe. The x-axis points from the IP to the centre of the LHC ring, and the y-axis points upwards. Polar coordinates (r, ϕ) are used in the transverse plane, ϕ being the azimuthal angle around the z-axis. The pseudorapidity is defined in terms of the polar angle θ as $\eta = -\ln\tan(\theta/2)$ and is equal to the rapidity $y = \frac{1}{2}\ln\left(\frac{E+p_z}{E-p_z}\right)$ in the relativistic limit. Angular distance is measured in units of $\Delta R \equiv \sqrt{(\Delta y)^2 + (\Delta\phi)^2}$.

JHEP10(2026)206

calorimetry is provided by the steel/scintillator-tile calorimeter, segmented into three barrel structures within $|\eta| < 1.7$, and two copper/LAr hadronic endcap calorimeters. The solid angle coverage is completed with forward copper/LAr and tungsten/LAr calorimeter modules optimised for electromagnetic and hadronic energy measurements, respectively.

The muon spectrometer (MS) comprises separate trigger and high-precision tracking chambers measuring the deflection of muons in a magnetic field generated by the superconducting air-core toroidal magnets. The field integral of the toroids ranges between 2.0 and 6.0 T m across most of the detector. Three layers of precision chambers, each consisting of layers of monitored drift tubes, cover the region $|\eta| < 2.7$, complemented by cathode-strip chambers in the forward region, where the background is highest. The muon trigger system covers the range $|\eta| < 2.4$ with resistive-plate chambers in the barrel, and thin-gap chambers in the endcap regions.

The luminosity is measured mainly by the LUCID–2 [28] detector that records Cherenkov light produced in the quartz windows of photomultipliers located close to the beampipe.

Events were selected by the first-level trigger system implemented in custom hardware, followed by selections made by algorithms implemented in software in the high-level trigger [29]. The first-level trigger accepted events from the 40 MHz bunch crossings at a rate close to 100 kHz, which the high-level trigger further reduced in order to record complete events to disk at about 1.25 kHz.

A software suite [30] is used in data simulation, in the reconstruction and analysis of real and simulated data, in detector operations, and in the trigger and data acquisition systems of the experiment.

3 Data and simulated event samples

The analysis uses 140 fb^{-1} of proton–proton (pp) collision data collected at $\sqrt{s} = 13$ TeV by the ATLAS experiment between 2015 and 2018, corresponding to the full LHC Run 2. Only events recorded under stable-beam conditions with all detector subsystems operating normally are included, and standard data-quality requirements are applied to ensure reliable reconstruction of physics objects [31]. The average number of simultaneous pp interactions per bunch crossing (pile-up) over the full dataset, $\langle\mu\rangle$, is approximately 34.

The search targets signal models in which a scalar mediator S is produced via gluon–gluon fusion and subsequently decays into a quasi-conformal hidden sector, following the framework described in section 1. The mediator is taken to be either the SM Higgs boson with mass $m_S = 125$ GeV, or a heavier scalar particle with $m_S = 400$ GeV or $m_S = 750$ GeV. The inclusion of heavier mediators allows the exploration of scenarios in which a larger total energy is injected into the hidden sector. The dark-meson mass is set to the benchmark values $m_\phi = 1.5$, 3, and 5 GeV, chosen as representative points within the range motivated in section 1. Consistent with the expectation that T is of the same order as m_ϕ, it is varied according to $T = \frac{2}{3}m_\phi$, $T = m_\phi$, and $T = \frac{3}{2}m_\phi$.

Representative benchmark scenarios for $m_{A'}$ are defined within the region that kinematically allows decays to muons. A dark-photon mass of $m_{A'} = 0.5$ GeV, corresponding to branching fractions $B(A' \to e^+e^-, \mu^+\mu^-, \pi^+\pi^-) = (0.4, 0.4, 0.2)$, is chosen as the nominal benchmark. This choice yields a substantial muon fraction while retaining a non-negligible

JHEP10(2026)206

m_S (GeV)	m_ϕ (GeV)	T (GeV)	$m_{A'}$ (GeV)
125	1.5	1.00, 1.50, 2.25	0.3, 0.5
125	3.0	2.0, 3.0, 4.5	0.5
125	5.0	3.33, 5.0, 7.5	0.3, 0.5
400	1.5	1.00, 1.50, 2.25	0.5, 0.7
400	3.0	2.0, 3.0, 4.5	0.5, 0.7
400	5.0	3.33, 5.0, 7.5	0.5, 0.7
750	1.5	1.00, 1.50, 2.25	0.5, 0.7
750	3.0	2.0, 3.0, 4.5	0.5, 0.7
750	5.0	3.33, 5.0, 7.5	0.5, 0.7

Table 1. Benchmark signal model parameters considered. When multiple comma-separated values are given, all combinations across columns of those parameters were generated.

contribution from hadronic decays, and all combinations of m_S, m_ϕ, and T are simulated for this benchmark. To probe the dependence on the final-state composition, two alternative benchmarks are considered. An enhanced-muon scenario with $m_{A'} = 0.3\,\text{GeV}$ and $B(A' \to e^+e^-, \mu^+\mu^-, \pi^+\pi^-) = (0.5, 0.5, 0.0)$ is studied for the case in which the mediator is the Higgs boson. In addition, a reduced-muon scenario with $m_{A'} = 0.7\,\text{GeV}$ and $B(A' \to e^+e^-, \mu^+\mu^-, \pi^+\pi^-) = (0.15, 0.15, 0.7)$ is considered for a subset of model-parameter combinations. A summary of the model parameters explored in this paper is shown in table 1. Not all combinations of model parameters were generated, and the selection balances the exploration of key model parameters and expectation of sensitivity to the chosen benchmarks.

Signal Monte Carlo (MC) samples are generated at leading order (LO) using Pythia 8.244.p3 [32] with the A14 tune [33] and the NNPDF2.3lo [34] parton distribution function (PDF) set. Their inclusive gluon-fusion production cross-section is set to the Next-to-Next-Leading-Order (NNLO) QCD calculations including exact next-to-leading-order (NLO) top-mass effects [35]. The Higgs boson decay is handled by a dedicated Pythia plug-in based on the model described in ref. [24], which models the quasi-conformal shower in the dark sector. The mediator branching ratio to the dark sector, $B(S \to \text{SUEP})$, is set to 100%. Dark photons are then decayed with the branching ratios reported above. The generated events are processed using a fast detector simulation based on a parameterization of the calorimeter response [36].

For signal models in which the mediator is the SM Higgs boson, events are reweighted to reproduce the NLO prediction for the Higgs boson transverse momentum spectrum, obtained from a sample generated with the Powheg Box v2 MC generator [37–41].

A $Z \to \mu^+\mu^-$ MC sample is used to calibrate both the trigger efficiency and the track multiplicity correction described in section 4. The Powheg Box v1 MC generator [39–42] was used for the simulation of the hard-scattering processes of Z-boson production at NLO in QCD, and for decaying it to the muon channel. It was interfaced to Pythia 8.186 [43] for the modeling of the parton shower, hadronization, and underlying event, with parameter values set according to the AZNLO tune [44]. The CT10nlo PDF set [45] was used for the hard-scattering processes, whereas the CTEQ6L1 PDF set [46] was used for the parton shower.

JHEP10(2026)206

The effect of additional photons in the final state was simulated with PHOTOS++ 3.52 [47, 48]. The EVTGEN 1.2.0 program [49] was used to decay bottom and charm hadrons.

Together with the $Z \to \mu^+\mu^-$ sample, MC samples of $t\bar{t}$, $t\bar{t}Z$ and diboson (VV) production are used to verify that only QCD multijet events are expected to contribute significantly to the search and validation regions defined in section 5. The production of $t\bar{t}$ events was modeled using the POWHEG BOX v2 [39–41, 50] generator at NLO with the NNPDF3.0NLO [34] PDF set and the h_{damp} parameter[2] set to $1.5\,m_{\text{top}}$ [51]. The events were interfaced to PYTHIA 8.230 [52] to model the parton shower, hadronization, and underlying event, with parameters set according to the A14 tune [33] and using the NNPDF2.3LO set of PDFs [53]. The decays of bottom and charm hadrons were performed by EVTGEN 1.6.0 [49].

The production of $t\bar{t}Z$ events was modeled using the MADGRAPH5_AMC@NLO 2.3.3 [54] generator at NLO with the NNPDF3.0NLO [34] PDF. The events were interfaced to PYTHIA 8.210 [52] using the A14 tune [33] and the NNPDF2.3LO [34] PDF set. The decays of bottom and charm hadrons were simulated using the EVTGEN 1.2.0 program [49].

Samples of diboson final states (VV) were simulated with the SHERPA 2.2.1 or 2.2.2 [55] generator depending on the process, including off-shell effects and Higgs boson contributions, where appropriate. Fully leptonic final states and semileptonic final states, where one boson decays leptonically and the other hadronically, were generated using matrix elements at NLO accuracy in QCD for up to one additional parton and at LO accuracy for up to three additional parton emissions. Samples for the loop-induced processes $gg \to VV$ were generated using LO-accurate matrix elements for up to one additional parton emission for both the cases of fully leptonic and semileptonic final states. The matrix element calculations were matched and merged with the SHERPA parton shower based on Catani–Seymour dipole factorization [56, 57] using the MEPS@NLO prescription [58–61]. The virtual QCD corrections were provided by the OPENLOOPS library [62–64]. The NNPDF3.0NNLO set of PDFs was used [34], along with the dedicated set of tuned parton-shower parameters developed by the SHERPA authors.

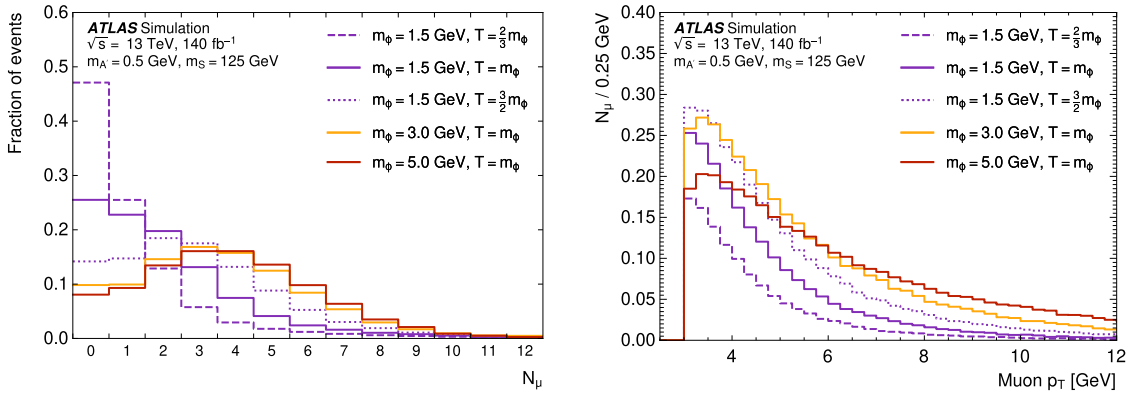
All background MC samples are processed using a full GEANT4-based detector simulation [36]. For all MC samples, pile-up was modeled by overlaying the simulated hard-scattering event with inelastic pp events generated with PYTHIA 8.186 [43] using the NNPDF2.3LO set of PDF [53] and the A3 set of tuned parameters [65]. All MC samples are reweighted such that the distribution of the number of pile-up vertices reproduces that observed in data.

4 Event reconstruction

Events are selected using the multi-muon trigger with the lowest p_{T} threshold that collected the full integrated luminosity in each data-taking period. This corresponds to a trigger requiring at least three muons with $p_{\text{T}} > 6\,\text{GeV}$ in 2015 and 2016, and at least four muons with $p_{\text{T}} > 4\,\text{GeV}$ in 2017 and 2018. Simulated signal samples are corrected to reproduce the trigger efficiency expected in data. A scale factor is applied to the simulated signal events, defined as the ratio of the trigger efficiency expected in data to that in simulation. Following ref. [66], the expected multi-muon trigger efficiency is estimated from the corresponding

[2]The h_{damp} parameter is a resummation damping factor and one of the parameters that controls the matching of POWHEG matrix elements to the parton shower and thus effectively regulates the high-p_{T} radiation against which the $t\bar{t}$ system recoils.

JHEP10(2026)206



(a) (b)

Figure 2. Expected reconstructed (a) muon multiplicity and (b) muon p_{T} spectrum, illustrating the dependence of these observables on the temperature T and dark-meson mass m_ϕ for a Higgs boson mediator and $m_{A'} = 0.5\,\mathrm{GeV}$, which corresponds to $B(A' \to e^+e^-, \mu^+\mu^-, \pi^+\pi^-) = (0.4,\, 0.4,\, 0.2)$. The muon selection requirements of the analysis are applied, but no event selection or trigger requirements.

single-muon trigger efficiencies with identical transverse momentum thresholds, assuming that the efficiencies for individual muons are uncorrelated.

The single-muon efficiencies are measured in data and in the $Z \to \mu^+\mu^-$ MC sample for muons passing the offline selection requirements, using a tag-and-probe method similar to that described in ref. [66]. In addition to the binning in η, ϕ, and data-taking period used in ref. [66], an additional binning in p_{T} is introduced to better model the reduced efficiency in the trigger turn-on region. The p_{T} bin edges are defined as $[4, 6, 8, 10, \infty)\,\mathrm{GeV}$. At least three (four) muons reconstructed by the High Level Trigger are required to be within $\Delta R = 0.07$ of an offline muon in 2015 and 2016 (2017 and 2018). The trigger efficiency ranges from approximately 1% for all signal models with $m_\phi = 1.5\,\mathrm{GeV}$ and $T = 1\,\mathrm{GeV}$ to nearly 100% for the model with $m_s = 750\,\mathrm{GeV}$, $m_{A'} = 0.5\,\mathrm{GeV}$, and $m_\phi = T = 5\,\mathrm{GeV}$. The corresponding scale factors range between 0.85 and 1. The variations in trigger efficiency and scale factor are driven by differences in the muon kinematics, in particular the p_{T} spectrum and multiplicity, between signal models. Figure 2 illustrates this dependence for muons passing the selection requirements detailed below, before any event selection is applied.

Events are required to have at least one reconstructed vertex [67] with at least two associated tracks with p_{T} larger than 500 MeV that are consistent with originating from the beam collision region. The vertex with the highest sum of squared transverse momenta of associated tracks is considered as the primary vertex (PV) of the event. The transverse and longitudinal impact parameters of all tracks, denoted by d_0 and z_0, respectively, are calculated relative to the beamline. For the longitudinal impact parameter, the z-position of the primary vertex is used as the reference point.

Muons are reconstructed by combining tracks in the ID with tracks in the MS in the range $|\eta| < 2.5$. They are required to have $p_{\mathrm{T}} > 3$ GeV and to satisfy the cut-based *LowPt* working point defined in ref. [68]. The combined tracks must also meet the requirements

JHEP10(2026)206

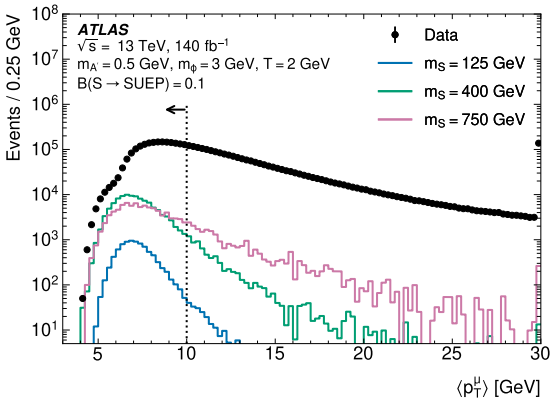


Figure 3. Average p_{T} of muons passing the selection requirements for events satisfying the trigger requirements. Data are compared with a range of signal models to illustrate the dependence on the scalar mediator mass. The shoulder observed around 7 GeV in data arises from the combination of multiple trigger selections. The dotted line and arrow indicate the region selected by the analysis. Overflow entries are included in the last bin.

$|d_0| < 2$ mm and $|\Delta z_0 \sin\theta| < 3$ mm, ensuring muons originate close to the PV and suppressing backgrounds with non-prompt decays from heavy-flavor hadrons.

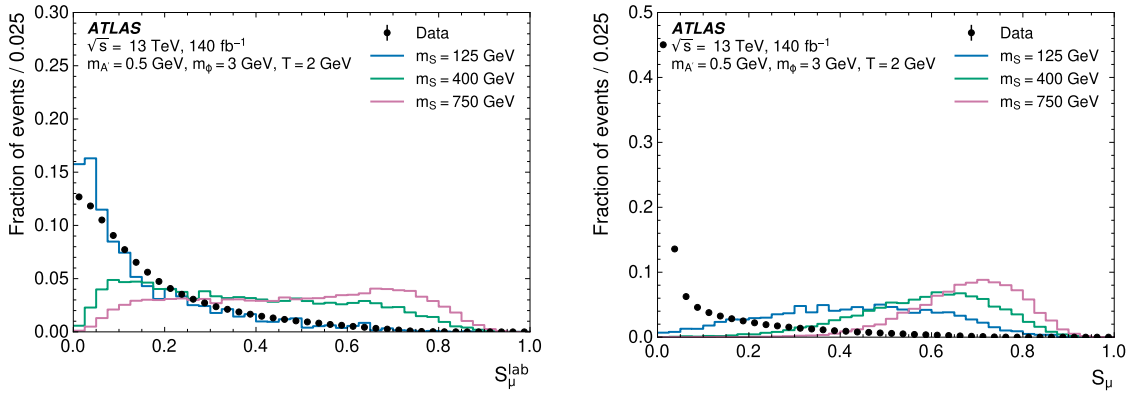
ID tracks are used to characterize the charged-particle activity in the event. These tracks include those associated with reconstructed muons as well as other charged particles. They must satisfy $p_{\mathrm{T}} > 0.5$ GeV, $|\eta| < 2.5$, $|d_0| < 0.5$ mm, and $|\Delta z_0 \sin\theta| < 0.5$ mm, ensuring they are within the ID acceptance, reconstructed by the track reconstruction algorithms, and compatible with originating at the PV.

Events are required to have an average muon transverse momentum $\langle p_{\mathrm{T}}^{\mu} \rangle < 10$ GeV, computed using all muons that pass the selection requirements. The distribution of $\langle p_{\mathrm{T}}^{\mu} \rangle$ for data and selected signal models is shown in figure 3. This requirement strongly suppresses backgrounds in which muons originate from the decays of heavy particles such as vector bosons or top quarks. According to simulation, after applying this requirement, the largest background contribution other than QCD multijet production arises from $t\bar{t}$ production and amounts to approximately 0.5% of events entering the search region, while contributions from $Z \to \mu^+\mu^-$, $t\bar{t}Z$, and VV processes are found to be at the level of 10^{-4} or smaller. Other processes involving heavy particles, such as $t\bar{t}W$, $t\bar{t}H$, and triboson production, are expected to contribute at a similar level. As a result, the background is dominated by QCD multijet events, where muons are predominantly produced in decays of heavy-flavor hadrons, as well as kaons and pions. As described in section 5, the background contribution is estimated using a likelihood-based ABCD method based on the muon sphericity S_{μ} and the track multiplicity N_{tracks}, defined below.

4.1 Sphericity

Sphericity is an event-shape observable used to characterize the geometrical properties of particle production in high-energy collisions [69]. It is typically computed using all reconstructed particles. In this analysis, it is instead constructed using only reconstructed muons.

JHEP10(2026)206



(a) (b)

Figure 4. Sphericity of muons (a) computed in the laboratory frame S_μ^{lab} and (b) computed after boosting to the muon-system rest frame S_μ for selected signal models and data. The distributions are shown for events passing the trigger selection requirement and with $\langle p_{\text{T}}^{\mu} \rangle < 10\,\text{GeV}$.

In signal events, the muons are approximately isotropically distributed in the rest frame of the mediator S, which is generally boosted in the laboratory frame, particularly for models with low m_S, m_ϕ, or T that rely on this boost to satisfy the trigger requirements. To reduce the impact of this boost, all muon four-momenta are first summed to define the total four-momentum of the system. A Lorentz transformation is performed to express the muon four-momenta in the rest frame of the system. In this frame, the spatial momentum components are used to build the quadratic momentum tensor,

$$S^{\alpha\beta} = \frac{\sum_i p_i^\alpha p_i^\beta}{\sum_i |\vec{p}_i|^2}, \tag{4.1}$$

where the sum runs over all selected muons and α, β denote spatial indices. The tensor is diagonalized to obtain its eigenvalues $\lambda_1 \geq \lambda_2 \geq \lambda_3$, which satisfy $\lambda_1 + \lambda_2 + \lambda_3 = 1$. The sphericity is then defined as

$$S_\mu = \frac{3}{2}(\lambda_2 + \lambda_3). \tag{4.2}$$

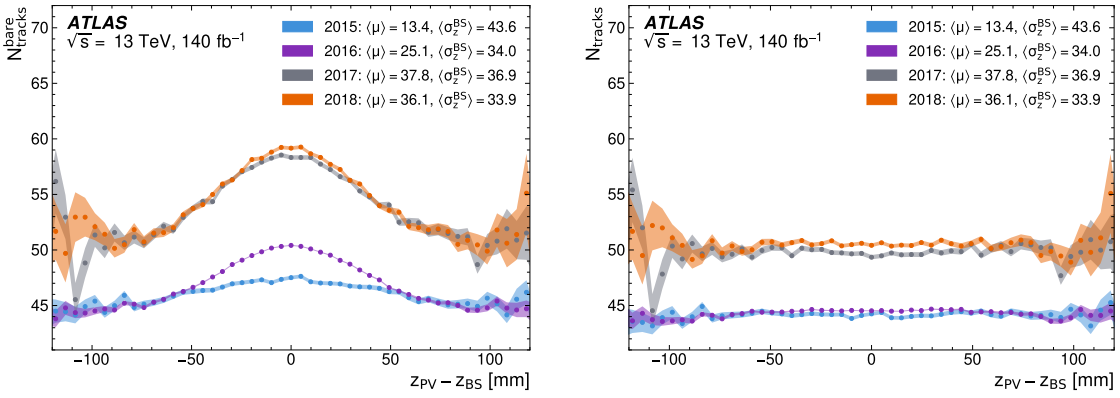
This observable takes values close to zero for very collimated configurations and approaches unity for isotropic configurations. As shown in figure 4, for signal models the value of S_μ is larger than that obtained when computed in the laboratory frame, while in data the S_μ distribution is shifted towards lower values compared to the laboratory-frame definition.

4.2 Track multiplicity

The number of reconstructed tracks is a powerful observable for discriminating signal from background. A large multiplicity of low-momentum muons, electrons,[3] and/or charged

[3]Electrons, which cannot be reliably reconstructed or identified in this analysis due to their low p_{T}, as well as muons that are below the minimum p_{T} specified in section 4, may still be reconstructed as charged-particle tracks.

JHEP10(2026)206



(a) (b)

Figure 5. (a) Bare and (b) corrected track multiplicities as a function of the longitudinal distance between the PV and the mean position of the luminous region, shown for different years of data-taking. The error bands indicate the statistical uncertainty.

hadrons (depending on the specific $m_{A'}$) is expected in the case of signal events, far exceeding what is typical in background processes.

The tight requirement on the longitudinal track impact parameter ($|\Delta z_0 \sin\theta| < 0.5$ mm) helps to isolate tracks originating from the hard-scattering interaction from those originating from pile-up interactions. However, pile-up interactions can still contribute when their vertices are sufficiently close to the PV. The size of this contribution depends on the local density of pile-up vertices near the PV and thus varies with data-taking conditions. This behavior is illustrated in figure 5(a), which shows that the increase in the bare (uncorrected) track multiplicity $N_{\text{tracks}}^{\text{bare}}$ for PVs near the longitudinal center of the luminous region (or beam spot) z_{BS} depends on the data-taking period, reflecting differences in the average number of pile-up interactions per bunch crossing μ and in the longitudinal width of the beam spot σ_z^{BS}. Additionally, significant uncertainties in the modeling of inelastic pp interactions affect the multiplicity and kinematic properties of charged particles produced in pile-up vertices.

To reduce the sensitivity of the analysis to these effects, a data-driven estimate of the average number of pile-up tracks passing the track selection is employed. Such an estimate is expected to depend on beam conditions at the time the event was recorded and denoted $N_{\text{tracks}}^{\text{PU}}$, and it is subtracted from $N_{\text{tracks}}^{\text{bare}}$ to define the corrected track multiplicity:

$$N_{\text{tracks}} = N_{\text{tracks}}^{\text{bare}} - N_{\text{tracks}}^{\text{PU}}((z_{\text{PV}} - z_{\text{BS}})/\sigma_z^{\text{BS}}, \mu), \tag{4.3}$$

where $N_{\text{tracks}}^{\text{PU}}$ is defined in eq. (4.4) and z_{PV} is the longitudinal position of the primary vertex of the event. The beam spot parameters z_{BS} and σ_z^{BS} are determined from fits to the spatial distribution of reconstructed primary vertices, accumulated over many events within a given time period of about 60 s [70], and μ is measured by the LUCID-2 detector [71] as an average over many bunch crossings.

The contribution $N_{\text{tracks}}^{\text{PU}}$ is estimated using tracks whose longitudinal impact parameter is consistent with originating away from the PV, where only pile-up contributions are expected. Figure 6 shows the track multiplicity as a function of the longitudinal displacement relative

JHEP10(2026)206

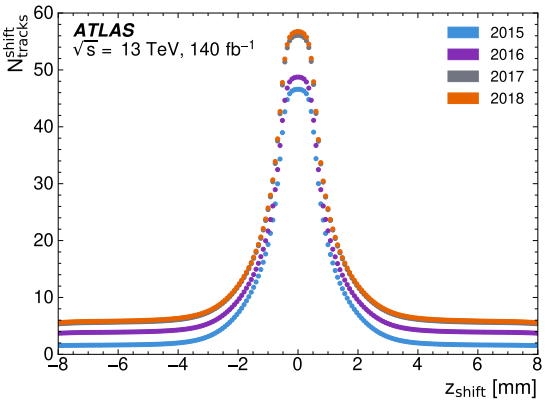


Figure 6. Multiplicity of tracks $N_{\text{tracks}}^{\text{shift}}$ when taken as a function of the track longitudinal impact parameters with respect to the PV (z_{shift}).

to the PV, denoted z_{shift}. The contribution from tracks originating from the PV becomes negligible for $|z_{\text{shift}}| \gtrsim 4$ mm, as indicated by the approximately flat distribution in these ranges. A mild decrease toward larger values of $|z_{\text{shift}}|$ is observed and expected, consistent with the reduced pile-up vertex density away from z_{BS}. The measurement of $N_{\text{tracks}}^{\text{PU}}$ is therefore performed by counting how many tracks are within a window of 1 mm around $z_{\text{shift}} = 6.5$ mm, using events that satisfy the trigger requirements.

The resulting track multiplicity is dependent on μ and on the location relative to the beamspot center, normalized by the beamspot width ($(z - z_{\text{BS}})/\sigma_z^{\text{BS}}$). The expected $N_{\text{tracks}}^{\text{PU}}$ at any given longitudinal position z can then be derived assuming a Gaussian dependence on $(z - z_{\text{BS}})/\sigma_z^{\text{BS}}$ and a linear dependence on μ:

$$N_{\text{tracks}}^{\text{PU}}((z - z_{\text{BS}})/\sigma_z^{\text{BS}}, \mu) = \mu\, A \exp\left[-\tfrac{1}{2}\left(\frac{(z - z_{\text{BS}})/\sigma_z^{\text{BS}}}{B}\right)^2\right] + N_0, \tag{4.4}$$

where A, B, and N_0 are determined from a χ^2 fit to the measured track multiplicities. The parameter N_0 accounts for additional contributions that are largely independent of μ and $(z - z_{\text{BS}})/\sigma_z^{\text{BS}}$. For consistency, the procedure is performed independently in data and simulation, using a $Z \to \mu^+\mu^-$ sample for the latter. The fitted parameters for both data and simulation are listed in table 2.

As shown in figure 5(b), the corrected observable N_{tracks} exhibits no significant dependence on the PV position within the beam spot or on variations in instantaneous luminosity. A residual difference between the 2015–2016 and 2017–2018 data-taking periods is observed and expected due to the different trigger selections employed during these periods, leading to a different average track multiplicity from the PV.

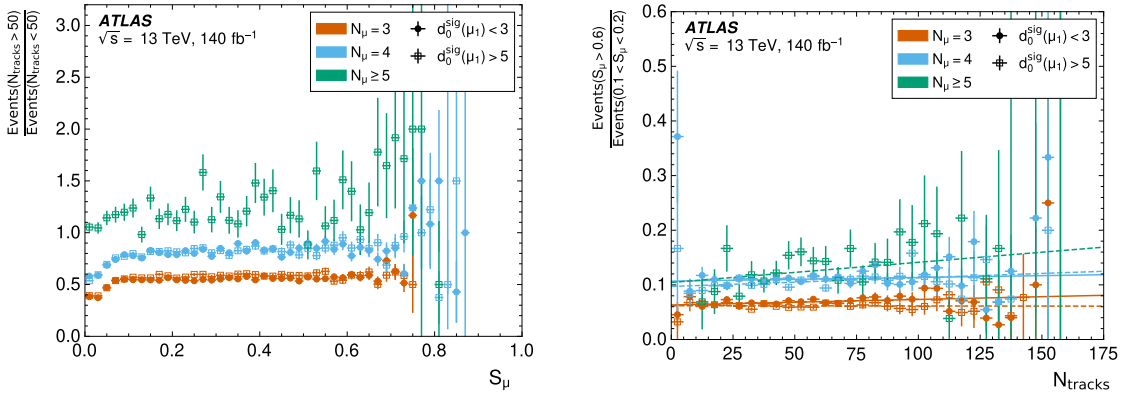
5 Event selection and background estimation

After the preselection requirement $\langle p_{\text{T}}^{\mu} \rangle < 10\,\text{GeV}$, the dominant background arises from QCD multijet events in which heavy-flavor hadrons decay into muons. While the signal is assumed to be prompt, heavy-flavor hadrons can have sizable lifetimes, resulting in displaced

JHEP10(2026)206

	A	B	N_0
Data	0.2240 ± 0.0006	0.9589 ± 0.0028	0.474 ± 0.005
MC	0.2072 ± 0.0006	0.9182 ± 0.0027	0.440 ± 0.005

Table 2. Fitted parameters of $N_{\text{tracks}}^{\text{PU}}$ for data and MC with $\pm 1\sigma$ fit uncertainties.



(a) (b)

Figure 7. (a) Ratio of the number of data events with $N_{\text{tracks}} > 50$ to those with $N_{\text{tracks}} < 50$ as a function of S_μ and (b) ratio of the number of data events with $S_\mu > 0.6$ to those with $0.1 < S_\mu < 0.2$ as a function of N_{tracks}, shown for each validation region. The solid (dashed) lines in the right panel indicate linear fits to the ratio for validation regions with $d_0^{\text{sig}}(\mu_1) < 3$ ($d_0^{\text{sig}}(\mu_1) > 5$).

muon signatures. The search region therefore requires the transverse impact-parameter significance of the highest-p_{T} muon, $d_0^{\text{sig}}(\mu_1) = \left|\frac{d_0(\mu_1)}{\sigma_{d_0}(\mu_1)}\right| < 3$, where μ_1 denotes the highest-p_{T} muon. In addition, a requirement on the muon multiplicity, $N_\mu \geq 5$, further suppresses the background. The selection efficiency of the requirements on $\langle p_{\text{T}}^\mu \rangle$, $d_0^{\text{sig}}(\mu_1)$, and N_μ is close to unity for all signal models.

Background events with displaced leptonic decays are not expected to differ significantly in topology from those entering the search region. Alternative requirements on $d_0^{\text{sig}}(\mu_1)$ and N_μ are therefore used to define regions in which the background estimation method is tested and validated. The selections defining the validation and search regions are summarized in table 3.

As illustrated in figure 7, N_{tracks} and S_μ are largely uncorrelated in the validation regions once the region $S_\mu < 0.1$ is excluded. This low-S_μ region is dominated by events in which muons are collimated into two narrow cones with well-aligned axes. Such topologies are predominantly expected in events without additional jet activity away from this axis, resulting in a significantly reduced N_{tracks} and a stronger correlation between N_{tracks} and S_μ. A small trend in the ratio of the number of events satisfying $S_\mu > 0.6$ to those with $0.1 < S_\mu < 0.2$ is observed, particularly pronounced in the validation region defined by $N_\mu \geq 5$ and $d_0^{\text{sig}}(\mu_1) > 5$. A dedicated systematic uncertainty is discussed in section 6 that takes this correlation into account.

Based on the assumption that the correlation between N_{tracks} and S_μ is similarly low in the search region, the background is modeled using a multi-bin likelihood-based ABCD

JHEP10(2026)206

Requirements		Region purpose
$N_\mu = 3$	$d_0^{\text{sig}}(\mu_1) > 5$	validation
	$d_0^{\text{sig}}(\mu_1) < 3$	validation
$N_\mu = 4$	$d_0^{\text{sig}}(\mu_1) > 5$	validation
	$d_0^{\text{sig}}(\mu_1) < 3$	validation
$N_\mu \geq 5$	$d_0^{\text{sig}}(\mu_1) > 5$	validation
	$d_0^{\text{sig}}(\mu_1) < 3$	search

Table 3. Definition of the validation and search regions.

method. The method allows a fully data-driven background prediction that does not rely on the simulated background samples. Events are categorized in a two-dimensional histogram of N_{tracks} and S_μ, as shown in figure 8. Along the N_{tracks} axis, the bin edges are defined at $(-\infty, 20, 40, 60, 80, 120, 170, \infty)$,[4] with each bin inclusive of its lower boundary. This binning is chosen to ensure good sensitivity across the full range of signal models considered, which show a wide variety of N_{tracks} distributions. The S_μ axis is partitioned into two disjoint intervals: $0.1 < S_\mu < 0.2$ and $S_\mu > 0.6$.

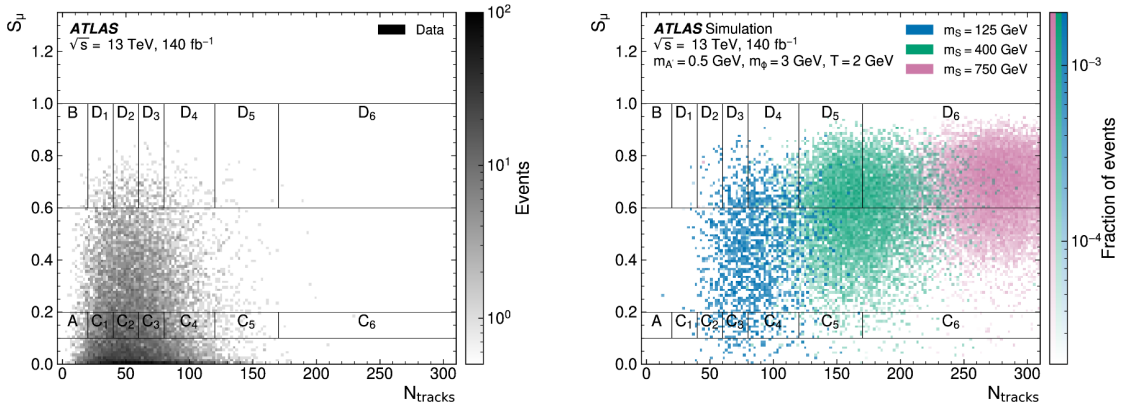
For increasing N_{tracks}, the bins in the low-S_μ interval are labelled A, $C_1, \ldots, C_6$, while the corresponding bins in the high-S_μ interval are labelled B, $D_1, \ldots, D_6$. In the search region, the background is expected to populate predominantly the control-region bins A, B, and $C_1, \ldots, C_6$, whereas signal events are expected to contribute primarily to the signal region bins $D_1, \ldots, D_6$.

The stringent requirement of $S_\mu > 0.6$ defining the signal-region bins is chosen to enhance the sensitivity of the search relative to looser S_μ selections. Conversely, the upper bound $S_\mu < 0.2$ for the control-region bins A, $C_1, \ldots, C_6$ is chosen to suppress potential contamination from certain signal models, allowing this region, together with the region B, to be unblinded during the development of the analysis strategy. Since including the intermediate region $0.2 < S_\mu < 0.6$ as additional signal-region bins does not improve the overall sensitivity, this region is excluded from the analysis entirely.

The background model is constrained using maximum-likelihood fits to data, as further detailed in section 7. When testing signal hypotheses, the likelihood includes a signal component, such that the background normalization parameters are determined simultaneously with the scale of the signal contribution. This procedure ensures a consistent determination of the background model both in background-only fits and in fits allowing for a potential signal contribution, including cases where non-negligible signal contributions are present in control-region bins.

[4] Negative N_{tracks} values can arise from the subtraction of the average expected pile-up contribution (section 4.2).

JHEP10(2026)206



(a) (b)

Figure 8. Binning of the N_{tracks}–S_μ histograms and distributions in the search region of (a) data and (b) selected signal models. The signal entries are normalized to unity. The signal region corresponds to the bins $D_1, \ldots, D_6$.

6 Systematic uncertainties

Experimental uncertainties on the simulated signal yields are evaluated to account for potential differences between data and simulated signal samples in the event reconstruction and selection. The relative importance of the various uncertainty sources depends strongly on the signal model parameters. For models with m_ϕ, $T \lesssim 3\,\text{GeV}$, where the acceptance is largely constrained by the p_{T} thresholds of the online muon reconstruction, the dominant contribution is expected to arise from the trigger efficiency. For models with m_ϕ, $T \gtrsim 3\,\text{GeV}$, uncertainties associated with ID tracking are expected to become largest. This behavior is reflected in the ranges quoted for the individual uncertainty sources below.

Two sources of systematic uncertainty affecting the trigger efficiency are evaluated, both arising from the tag–and–probe procedure used to determine the single-muon trigger efficiencies. The first originates from the limited statistical precision of the measurement, with its impact on the signal yield in the search region ranging from about 0.1% to 20%, depending on the model parameters. The second is derived by varying the selection requirements applied to the probe muon. The set of variations follows ref. [66], except for the probe-muon p_{T} requirement, which is adapted to accommodate the additional p_{T} binning used. The effect of this second source on the signal yield in the search region ranges from roughly 0.1% to 4%, depending on the model parameters.

Offline muon reconstruction is affected by uncertainties in the resolution of the combined muon track and in the reconstruction efficiency. The impact of the muon track-resolution uncertainty is found to be negligible. The uncertainty associated with the mismodeling of the muon reconstruction efficiency leads to variations in the signal yield in the search region ranging from approximately 0.5% to 5%, depending on the model parameters.

An uncertainty of 100% is assigned to the estimated rate of tracks arising from combinatorial background in the ID, based on comparisons between data and simulation of the reconstructed track multiplicity as a function of pile-up [67]. Since the contribution of such

JHEP10(2026)206

tracks is small, its effect on N_{tracks} ranges from approximately 1% to 5%, depending on the model parameters. For models predicting very high N_{tracks}, this uncertainty is largest in relative terms; however, its impact on the search sensitivity is sub-dominant, since all events remain within the highest N_{tracks} bin under any variation. Uncertainties on the ID track-resolution and reconstruction-efficiency modeling are found to be negligible for all signal models.

A pile-up modeling uncertainty is assigned to account for the difference between the predicted and measured inelastic cross-sections [72]. Its effect is evaluated to be below 3% on the signal yield in the search region and below 1% on N_{tracks} for all signal models.

An uncertainty on $N_{\text{tracks}}^{\text{PU}}$ is evaluated by repeating the measurement using either an alternative $Z \to \mu^+\mu^-$-enriched event selection or alternative offsets of $z_{\text{shift}} = -6.5$ mm and $z_{\text{shift}} = 7$ mm. The envelope of the variations is taken as the $\pm 1\sigma$ uncertainty. The impact of this uncertainty on N_{tracks} is found to be below 0.5% for all signal models.

For signal models in which the mediator is the Higgs boson, acceptance uncertainties are evaluated by varying the renormalization and factorization scales, PDF eigenvectors and PDF sets, parton shower settings, and by comparing the nominal NLO Higgs p_{T} spectrum prediction with an alternative NNLO prediction and its variations. The combined uncertainty from these sources is evaluated to be 20% and is applied to the expected signal yields in the D_i bins.

The uncertainty on the combined 2015–2018 integrated luminosity is 0.83% [71], derived using the LUCID-2 detector [28] for the primary luminosity measurements.

The statistical uncertainty of the regions used to estimate the background is propagated as a systematic uncertainty on the prediction. Additionally, a systematic uncertainty of 5–10% is assigned to the background yields in the D_i bins to account for the sensitivity of the prediction to the definition of the control regions. This uncertainty is evaluated by varying both the lower and upper S_μ boundaries of the A and C_i bins by ± 0.01, corresponding to small changes around the nominal region.

As illustrated in figure 7, the ratio of the number of events satisfying $S_\mu > 0.6$ to those with $0.1 < S_\mu < 0.2$ increases slightly with increasing N_{tracks}. This trend is particularly pronounced in the validation region defined by $N_\mu \geq 5$ and $d_0^{\text{sig}}(\mu_1) > 5$. To account for this residual correlation, a systematic uncertainty is introduced that allows the background model to deviate from the assumption of independence between N_{tracks} and S_μ. The size of this uncertainty is determined from the validation regions by fitting the ratio shown in figure 7 with a linear function in each validation region and taking the largest observed deviation from the expectation of no correlation, corresponding to a zero slope (see section 7 for details on its implementation and impact). Several possible sources of this positive correlation have been investigated. Those include slightly different composition in exclusive muon-multiplicity bins compared with the inclusive five or more muons required in the signal region, a data-taking time dependence due to slightly different triggers active in 2015–2016 compared to 2017–2018, contributions from decays in flight of light charged hadrons (which were found to increase with the muon multiplicity), and effects of correlated muon production through resonances as in $J/\psi \to \mu^+\mu^-$ decays. None of these effects alone could fully explain the observed correlation, although each contributed to some extent.

JHEP10(2026)206

7 Statistical analysis and results

The statistical interpretation is based on profile-likelihood-ratio test statistics. The goodness of fit of the background-only model is evaluated using a likelihood-ratio test with respect to a model that perfectly describes the observed data, while each signal hypothesis is tested using profile-likelihood ratios comparing the background-only and signal-plus-background hypotheses. In all cases, p-values are computed using asymptotic approximations [73].

To account for the systematic uncertainty associated with the residual correlation between N_{tracks} and S_μ, described in section 6, the following relations are imposed on the expected background yields b_r in bin r:

$$\begin{aligned} b_A &= \mu_A, \\ b_B &= \mu_A \epsilon_{AB} \left(1 + \chi \langle N_{\text{tracks}} \rangle_B\right), \\ b_{C_i} &= \mu_A \epsilon_i, \\ b_{D_i} &= \mu_A \epsilon_{AB} \epsilon_i \left(1 + \chi \langle N_{\text{tracks}} \rangle_{D_i}\right), \qquad \forall\, i \in \{1, \ldots, 6\}, \end{aligned} \tag{7.1}$$

where μ_A, ϵ_{AB}, and ϵ_i are normalization parameters, $\langle N_{\text{tracks}} \rangle_r$ denotes the average value of N_{tracks} in bin r, and χ is a single, Gaussian-distributed nuisance parameter with mean zero (corresponding to the no-correlation case) and standard deviation σ_χ, set as described below.

The parameter χ allows deviations from the assumption that the ratios $\frac{b_B}{b_A}$ and $\frac{b_{D_i}}{b_{C_i}}$ are equal. It captures a small linear dependence of these ratios on N_{tracks} that is characteristic of the background and not typically reproduced by potential signal contributions. To determine σ_χ, linear fits to the ratio of the number of events with $S_\mu > 0.6$ to those with $0.1 < S_\mu < 0.2$ as a function of N_{tracks} are performed in the validation regions, as illustrated in figure 7. The value $\sigma_\chi = 0.0036$ is taken as the ratio of the slope to the intercept obtained from the fit in the validation region defined by the requirements $N_\mu \geq 5$ and $d_0^{\text{sig}}(\mu_1) > 5$, where the slope is largest.

Figure 9 shows the comparison between data and the background model obtained from background-only fits performed in two representative validation regions. The goodness-of-fit p-values for the background-only fits range from 0.48 (for $N_\mu \geq 5$, $d_0^{\text{sig}}(\mu_1) > 5$) to 0.92, indicating good agreement between data and the background model.

The distributions observed in data and the background predictions obtained from background-only fits in the search region are shown in figure 10. While a mild excess of events in the highest N_{tracks} bin is observed, the fit yields a goodness-of-fit p-value of 0.42, indicating good overall agreement between the background-only hypothesis and the data. The two observed events in the region D_6 have (N_{tracks}, N_μ, S_μ) = (188, 5, 0.63) and (173, 7, 0.68), respectively. The result of a signal-plus-background fit in the search region is shown in figure 11. The fit includes the signal model with $m_S = 400\,\text{GeV}$, $m_{A'} = 0.7\,\text{GeV}$, $m_\phi = 3\,\text{GeV}$, and $T = 3\,\text{GeV}$, which can partially accommodate the excess, leading to a local significance of 1.7σ,[5] the largest observed among all tested signal models.

The parameter χ is fitted to $+1.5\sigma_\chi$ in the background-only fit. In signal-plus-background fits, χ is negatively correlated with the signal strength for signal hypotheses that can partially

[5]The quoted local significance, computed using asymptotic approximations, is found to be consistent with a calculation based on toy experiments.

JHEP10(2026)206

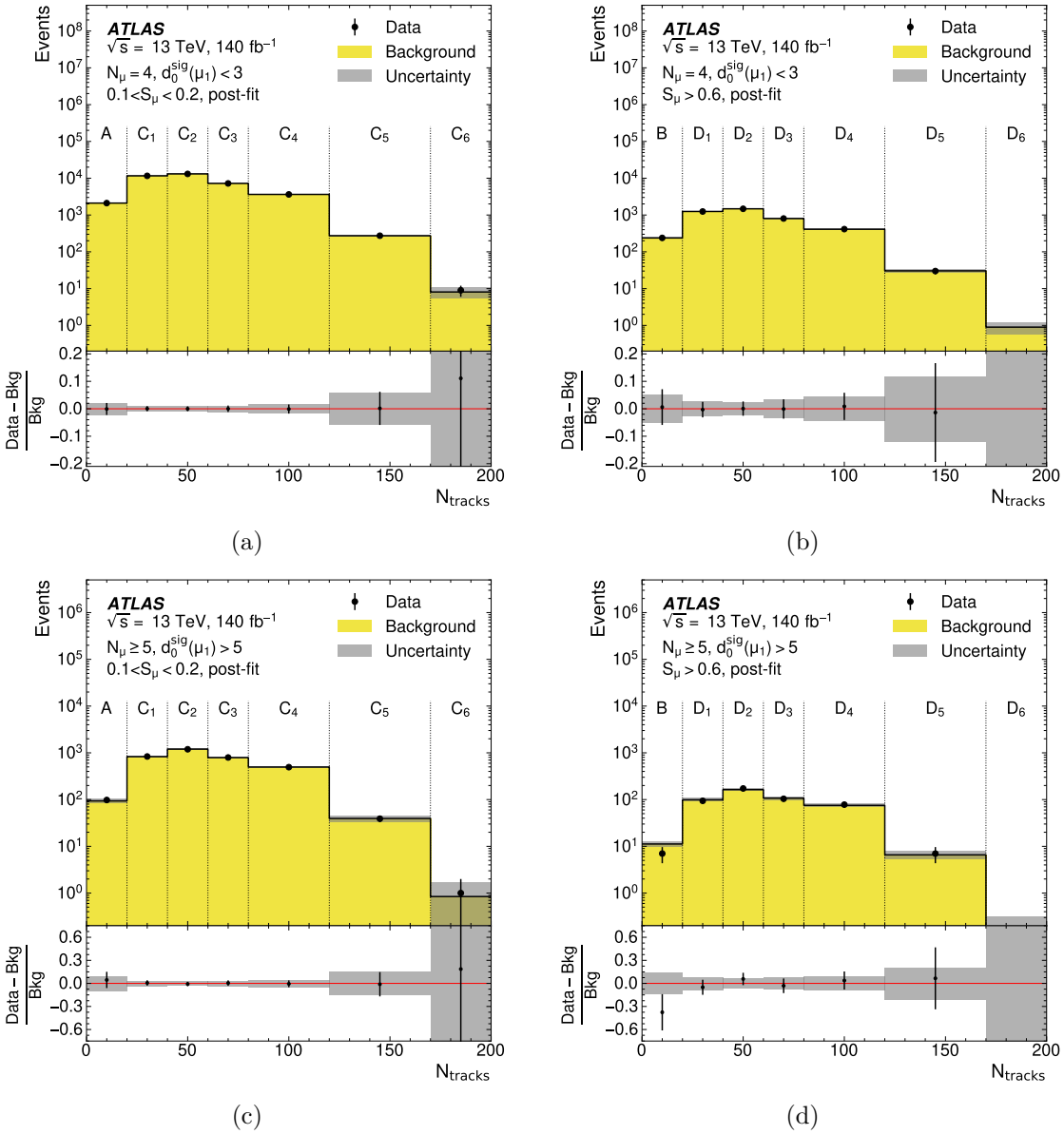


Figure 9. Background-only fits in the validation regions with requirements ((a),(b)) $d_0^{\text{sig}}(\mu_1) < 3$ and $N_\mu = 4$, and ((c),(d)) $d_0^{\text{sig}}(\mu_1) > 5$ and $N_\mu \geq 5$,. The N_{tracks} distributions are shown for ((a),(c)) $0.1 < S_\mu < 0.2$ and ((b),(d)) $S_\mu > 0.6$, with underflow and overflow entries included in the first and last bins, respectively. The background prediction (post-fit) includes the systematic uncertainties related to the estimation method described in section 6.

accommodate the excess. For the signal model with the largest local significance, the correlation coefficient is -0.3, and the fitted value of χ is reduced to $+1.0\sigma_\chi$.

Given that no significant deviation from the background-only hypothesis is observed, upper limits at the 95% confidence level (CL) are set on the product of the mediator production cross section and the branching fraction for its decay into a SUEP, $\sigma_S \times B(S \to \text{SUEP})$, using the CL_s method [74]. The results are shown in figure 12. Because of the mild excess

JHEP10(2026)206

observed in the highest N_{tracks} bin, the observed limits are slightly weaker than the expected limits, except for signal models predicting lower N_{tracks} values.

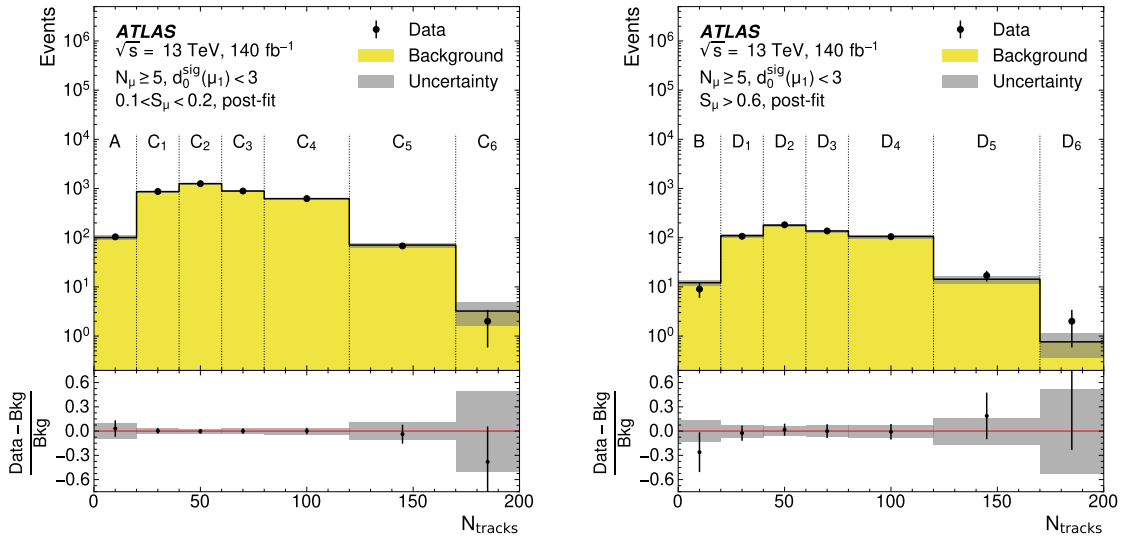
The limits reach values as low as approximately 0.05 fb for $m_S = 750\,\text{GeV}$, 0.4 fb for $m_S = 400\,\text{GeV}$, and 70 fb for $m_S = 125\,\text{GeV}$. Similarly, these limits can be interpreted as bounds on $B(S \to \text{SUEP})$. In the case of $m_S = 125\,\text{GeV}$, this corresponds to an upper limit on the Higgs boson branching fraction of around 0.2%, which is well below the limits on the invisible branching fraction obtained in model-independent searches [75].

The strongest limits are generally obtained for $m_\phi = T = 3\,\text{GeV}$, with reduced sensitivity at both lower and higher values of m_ϕ and T. For $m_\phi = T \approx 3\,\text{GeV}$, the trigger efficiency is high while the separation between signal and background in N_{tracks} remains strong. At lower values, the efficiency is reduced due to softer final-state particles, while at higher values the particle multiplicity decreases, leading to reduced discrimination power.

The sensitivity is higher for $m_{A'} = 0.5\,\text{GeV}$, which corresponds to branching fractions $B(A' \to e^+e^-, \mu^+\mu^-, \pi^+\pi^-) = (0.4, 0.4, 0.2)$, than for $m_{A'} = 0.7\,\text{GeV}$, where the muon branching fraction is reduced to 0.15. The improvement for $m_{A'} = 0.3\,\text{GeV}$, with a muon branching fraction of 0.5, is less pronounced.

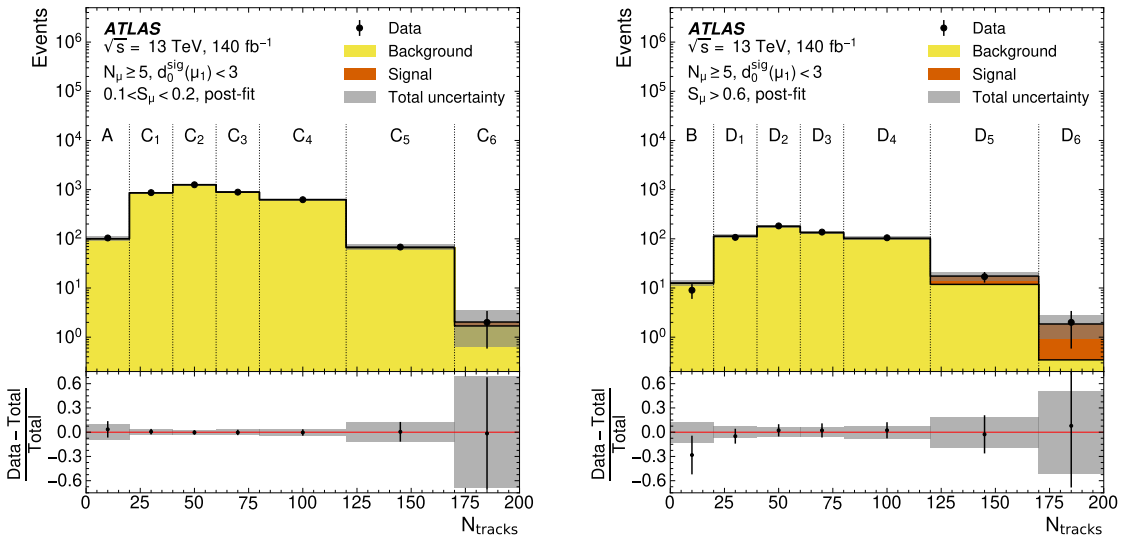
Taking $m_\phi = T = 3\,\text{GeV}$ and $m_{A'} = 0.5\,\text{GeV}$ as an example, the observed upper limits on the mediator production cross section via gluon–gluon fusion for the probed mediator masses are between one and four orders of magnitude more stringent than previous results [19]. Likewise, assuming the 125 GeV mediator is the SM Higgs boson, the upper limit on $B(H \to \text{SUEP})$ is around 0.3% for $m_\phi = T = 3, 5\,\text{GeV}$ and $m_{A'} = 0.5\,\text{GeV}$, which significantly improves upon those reported for similar model parameters in refs. [19, 20]. Overall, the benchmark models studied in this analysis show significant improvements over the results reported in refs. [19, 20] for the full range of $m_{A'}$ between 0.3 and 0.7 GeV.

JHEP10(2026)206



(a) (b)

Figure 10. Background-only fit in the search region defined by $N_\mu \geq 5$ and $d_0^{\text{sig}}(\mu_1) < 3$. The N_{tracks} distributions are shown for (a) $0.1 < S_\mu < 0.2$ and (b) $S_\mu > 0.6$, with underflow and overflow entries included in the first and last bins, respectively. The background prediction (post-fit) includes the systematic uncertainties related to the estimation method described in section 6.



(a) (b)

Figure 11. Signal-plus-background fit in the search region defined by $N_\mu \geq 5$ and $d_0^{\text{sig}}(\mu_1) < 3$ for the signal model with $m_S = 400\,\text{GeV}$, $m_{A'} = 0.7\,\text{GeV}$, $m_\phi = 3\,\text{GeV}$, and $T = 3\,\text{GeV}$. The N_{tracks} distributions are shown for (a) $0.1 < S_\mu < 0.2$ and (b) $S_\mu > 0.6$, with underflow and overflow entries included in the first and last bins, respectively. The background prediction (post-fit) includes the systematic uncertainties related to the estimation method described in section 6. The lower panels show the relative difference between data and the total fitted expectation (signal plus background). The fitted $\sigma_S \times B(S \to \text{SUEP})$ is 1.64 fb.

JHEP10(2026)206

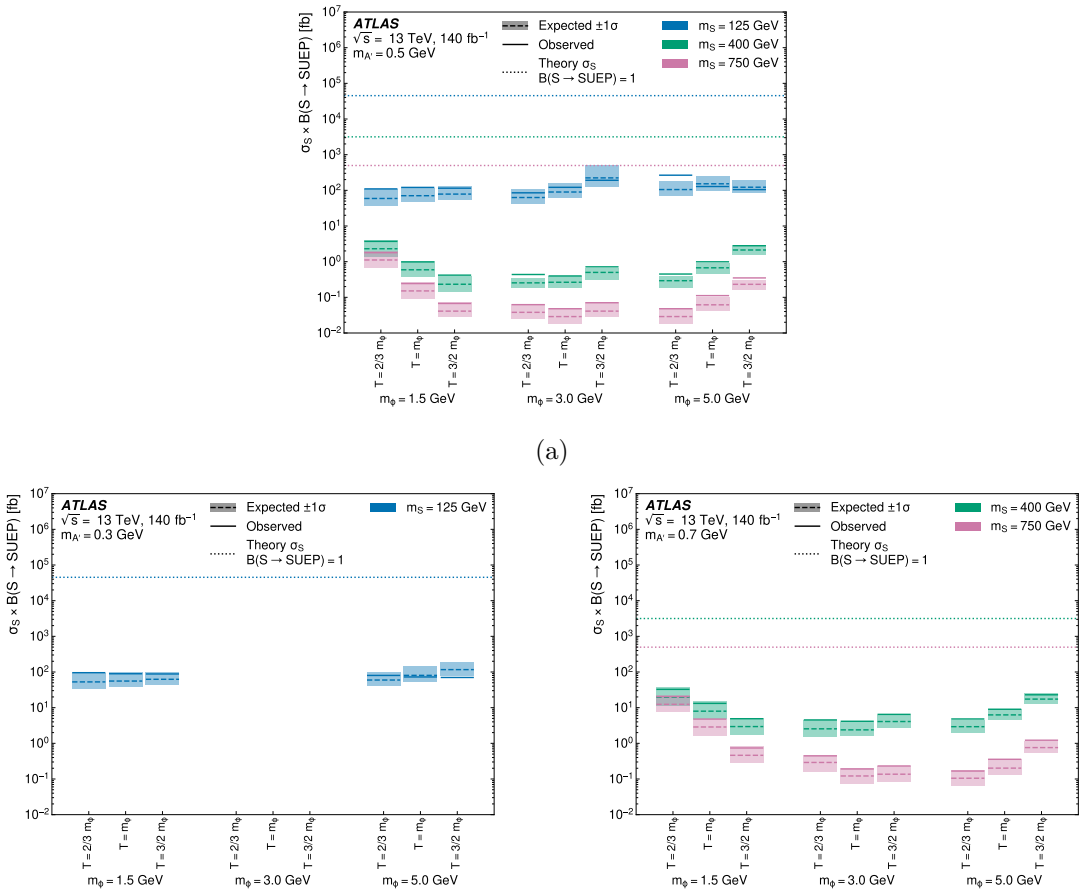


Figure 12. Expected and observed 95% CL upper limits on $\sigma_S \times B(S \to \text{SUEP})$ for models with (a) $m_{A'} = 0.5\,\text{GeV}$, (b) $m_{A'} = 0.3\,\text{GeV}$, and (c) $m_{A'} = 0.7\,\text{GeV}$. The theoretical predictions correspond to SM-like gluon-fusion production, as given in ref. [35]. The benchmark signal models shown for each value of $m_{A'}$ correspond to all tested signal models listed in table 1.

JHEP10(2026)206

8 Conclusion

A search for soft unclustered energy patterns is presented using 140 fb^{-1} of $\sqrt{s} = 13\,\text{TeV}$ proton–proton collision data recorded by the ATLAS detector. The analysis targets scenarios in which a scalar mediator decays into a strongly interacting, quasi-conformal hidden sector, giving rise to high-multiplicity final states containing low-momentum particles, including muons, that are distributed approximately isotropically in the mediator center-of-mass frame.

Events are selected using multi-muon triggers, and the search region is defined by requirements on the muon multiplicity, average muon transverse momentum, and transverse impact-parameter significance, targeting prompt, high-multiplicity final states with soft muons. The discrimination between signal and the dominant QCD multijet background is achieved using two observables: the muon sphericity, constructed in the rest frame of the muon system, and the charged-particle track multiplicity, corrected for pile-up. The background contribution is estimated by using a likelihood-based ABCD method that exploits the weak correlation between these observables, with residual correlations accounted for through a data-driven parameterization.

No significant deviation from the background-only hypothesis is observed in the search region. The results are therefore interpreted in terms of upper limits at the 95% confidence level on the product of the mediator production cross section and the branching fraction for its decay into a SUEP.

This search extends the sensitivity to SUEP scenarios beyond previous LHC results [19, 20], particularly in regions of parameter space characterized by moderate particle multiplicities and sizable muon fractions in the final state. The analysis demonstrates the effectiveness of multi-muon-based strategies and provides a complementary approach to existing searches targeting primarily hadronic final states.

Acknowledgments

We thank CERN for the very successful operation of the LHC and its injectors, as well as the support staff at CERN and at our institutions worldwide without whom ATLAS could not be operated efficiently.

The crucial computing support from all WLCG partners is acknowledged gratefully, in particular from CERN, the ATLAS Tier-1 facilities at TRIUMF/SFU (Canada), NDGF (Denmark, Norway, Sweden), CC-IN2P3 (France), KIT/GridKA (Germany), INFN-CNAF (Italy), NL-T1 (Netherlands), PIC (Spain), RAL (U.K.) and BNL (U.S.A.), the Tier-2 facilities worldwide and large non-WLCG resource providers. Major contributors of computing resources are listed in ref. [76].

We gratefully acknowledge the support of ANPCyT, Argentina; YerPhI, Armenia; ARC, Australia; BMWFW and FWF, Austria; ANAS, Azerbaijan; CNPq and FAPESP, Brazil; NSERC, NRC and CFI, Canada; CERN; ANID, Chile; CAS, MOST, NSFC and FRFCU, China; Minciencias, Colombia; MEYS CR, Czech Republic; DNRF and DNSRC, Denmark; IN2P3-CNRS and CEA-DRF/IRFU, France; SRNSFG, Georgia; BMFTR, HGF and MPG, Germany; GSRI, Greece; RGC and Hong Kong SAR, China; ICHEP and Academy of Sciences and Humanities, Israel; INFN, Italy; MEXT and JSPS, Japan; CNRST, Morocco; NWO,

JHEP10(2026)206

Netherlands; RCN, Norway; MNiSW, Poland; FCT, Portugal; MNE/IFA, Romania; MSTDI, Serbia; MSSR, Slovakia; ARIS and MVZI, Slovenia; DSI/NRF, South Africa; MICIU/AEI, Spain; SRC and Wallenberg Foundation, Sweden; SERI, SNSF and Cantons of Bern and Geneva, Switzerland; NSTC, Taipei; TENMAK, Türkiye; STFC/UKRI, United Kingdom; DOE and NSF, United States of America.

Individual groups and members have received support from BCKDF, CANARIE, CRC and DRAC, Canada; CERN-CZ, FORTE and PRIMUS, Czech Republic; COST, ERC, ERDF, Horizon 2020 and Marie Skłodowska-Curie Actions, European Union; Investissements d'Avenir Labex, Investissements d'Avenir Idex and ANR, France; DFG and AvH Foundation, Germany; Herakleitos, Thales and Aristeia programmes co-financed by EU-ESF and the Greek NSRF, Greece; BSF-NSF and MINERVA, Israel; NCN and NAWA, Poland; La Caixa Banking Foundation, CERCA and AGAUR programs from Generalitat de Catalunya and PROMETEO and GenT Programmes Generalitat Valenciana, Spain; Göran Gustafssons Stiftelse, Sweden; The Royal Society and Leverhulme Trust, United Kingdom; Eric and Wendy Schmidt Fund for Strategic Innovation, United States of America.

In addition, individual members wish to acknowledge support from Chile: Agencia Nacional de Investigación y Desarrollo (ANID FONDECYT reg. 1230987, FONDECYT 1230812, FONDECYT 1240864, Fondecyt 3240661, Fondecyt Regular 1240721); China: Fundamental Research Funds for the Central Universities (010-63263105), Chinese Ministry of Science and Technology (MOST-2023YFA1605700, MOST-2023YFA1609300), National Natural Science Foundation of China (NSFC 12275265, NSFC-W2543005); Czech Republic: Czech Science Foundation (GACR – 24-11373S), Ministry of Education Youth and Sports (ERC-CZ-LL2327, FORTE CZ.02.01.01/00/22_008/0004632); EU: H2020 European Research Council (ERC – 101002463); European Union: European Research Council (BARD No. 101116429, ERC – 101219398, ERC 101089007), European Regional Development Fund (HE COFUND GA No.101081355, ERDF), Marie Sklodowska-Curie Actions (GAP-101168829); France: Agence Nationale de la Recherche (ANR-21-CE31-0013, ANR-22-EDIR-0002, ANR-24-CE31-0504-01); Germany: Deutsche Forschungsgemeinschaft (DFG – 469666862); China: Research Grants Council (GRF); Italy: Istituto Nazionale di Fisica Nucleare (LHC-MIUR – 28003/2025), Ministero dell'Università e della Ricerca (NextGenEU I53D23000820006 M4C2.1.1, SOE2024_0000023); Japan: Japan Society for the Promotion of Science (JSPS KAKENHI JP25H0063, JSPS KAKENHI JP22H04944, JSPS KAKENHI JP24K23939, JSPS KAKENHI JP24KK0251, JSPS KAKENHI JP25H00650, JSPS KAKENHI JP25H01291, JSPS KAKENHI JP25K01011, JSPS KAKENHI JP25K01023, JSPS KAKENHI JP25KK0047); Poland: Polish National Science Centre (NCN 2021/42/E/ST2/00350, NCN OPUS 2023/51/B/ST2/02507, NCN OPUS nr 2022/47/B/ST2/03059, NCN UMO-2019/34/E/ST2/00393, UMO-2022/47/O/ST2/00148, UMO-2023/49/B/ST2/04085, UMO-2023/51/B/ST2/00920, UMO-2024/53/N/ST2/00869); Spain: Agència de Gestió d'Ajuts Universitaris i de Recerca. (AGAUR – 2023 BP 00141), Ministry of Science and Innovation (RYC2019-028510-I, RYC2020-030254-I, RYC2021-031273-I, RYC2022-038164-I), Ministerio de Ciencia, Innovación y Universidades/Agencia Estatal de Investigación (EU NextGenerationEU (PRTR-C17.I1), PID2022-142604OB-C22); Sweden: Carl Trygger Foundation (Carl Trygger Foundation CTS 22:2312), Swedish Research Council (Swedish Research Council

2023-04654, VR 2021-03651, VR 2022-03845, VR 2022-04683, VR 2023-03403, VR 2024-05451, VR 2025-05940), Knut and Alice Wallenberg Foundation (KAW 2023.0366); United Kingdom: The Binks Trust, Royal Society (NIF-R1-231091); United States of America: U.S. Department of Energy (ECA DE-AC02-76SF00515), John Templeton Foundation (John Templeton Foundation 63206), Neubauer Family Foundation.

Data Availability Statement. This article has no associated data or the data will not be deposited.

Code Availability Statement. This article has no associated code or the code will not be deposited.

Open Access. This article is distributed under the terms of the Creative Commons Attribution License (CC-BY4.0), which permits any use, distribution and reproduction in any medium, provided the original author(s) and source are credited.

JHEP10(2026)206

References

[1] M.J. Strassler and K.M. Zurek, *Discovering the Higgs through highly-displaced vertices*, *Phys. Lett. B* **661** (2008) 263 [hep-ph/0605193] [INSPIRE].

[2] M.J. Strassler and K.M. Zurek, *Echoes of a hidden valley at hadron colliders*, *Phys. Lett. B* **651** (2007) 374 [hep-ph/0604261] [INSPIRE].

[3] Z. Chacko, H.-S. Goh and R. Harnik, *The twin Higgs: Natural electroweak breaking from mirror symmetry*, *Phys. Rev. Lett.* **96** (2006) 231802 [hep-ph/0506256] [INSPIRE].

[4] D.E. Kaplan, M.A. Luty and K.M. Zurek, *Asymmetric Dark Matter*, *Phys. Rev. D* **79** (2009) 115016 [arXiv:0901.4117] [INSPIRE].

[5] Y. Bai and P. Schwaller, *Scale of dark QCD*, *Phys. Rev. D* **89** (2014) 063522 [arXiv:1306.4676] [INSPIRE].

[6] B.D. Wandelt et al., *Selfinteracting dark matter*, in the proceedings of the *4th International Symposium on Sources and Detection of Dark Matter in the Universe (DM 2000)*, Marina del Rey, U.S.A., 23–25 February 2000 [astro-ph/0006344] [INSPIRE].

[7] M. Rocha et al., *Cosmological Simulations with Self-Interacting Dark Matter I: Constant Density Cores and Substructure*, *Mon. Not. Roy. Astron. Soc.* **430** (2013) 81 [arXiv:1208.3025] [INSPIRE].

[8] S. Tulin and H.-B. Yu, *Dark Matter Self-interactions and Small Scale Structure*, *Phys. Rept.* **730** (2018) 1 [arXiv:1705.02358] [INSPIRE].

[9] CMS collaboration, *Search for resonant production of strongly coupled dark matter in proton-proton collisions at 13 TeV*, *JHEP* **06** (2022) 156 [arXiv:2112.11125] [INSPIRE].

[10] ATLAS collaboration, *Search for non-resonant production of semi-visible jets using Run 2 data in ATLAS*, *Phys. Lett. B* **848** (2024) 138324 [arXiv:2305.18037] [INSPIRE].

[11] ATLAS collaboration, *Search for new physics in final states with semivisible jets or anomalous signatures using the ATLAS detector*, *Phys. Rev. D* **112** (2025) 012021 [arXiv:2505.01634] [INSPIRE].

[12] CMS collaboration, *Search for dark QCD with emerging jets in proton-proton collisions at* $\sqrt{s} = 13$ *TeV*, *JHEP* **07** (2024) 142 [arXiv:2403.01556] [INSPIRE].

[13] ATLAS collaboration, *Search for emerging jets in pp collisions at* $\sqrt{s} = 13.6$ *TeV with the ATLAS experiment*, *Rept. Prog. Phys.* **88** (2025) 097801 [arXiv:2505.02429] [INSPIRE].

[14] M.J. Strassler, *Why Unparticle Models with Mass Gaps are Examples of Hidden Valleys*, arXiv:0801.0629 [INSPIRE].

[15] J. Polchinski and M.J. Strassler, *Deep inelastic scattering and gauge/string duality*, *JHEP* **05** (2003) 012 [hep-th/0209211] [INSPIRE].

[16] S. Lin and E. Shuryak, *Toward the AdS/CFT gravity dual for high energy collisions. II. The stress tensor on the boundary*, *Phys. Rev. D* **77** (2008) 085014 [arXiv:0711.0736] [INSPIRE].

[17] D.M. Hofman and J. Maldacena, *Conformal collider physics: Energy and charge correlations*, *JHEP* **05** (2008) 012 [arXiv:0803.1467] [INSPIRE].

[18] S. Knapen, S. Pagan Griso, M. Papucci and D.J. Robinson, *Triggering Soft Bombs at the LHC*, *JHEP* **08** (2017) 076 [arXiv:1612.00850] [INSPIRE].

[19] CMS collaboration, *Search for Soft Unclustered Energy Patterns in Proton-Proton Collisions at 13 TeV*, *Phys. Rev. Lett.* **133** (2024) 191902 [arXiv:2403.05311] [INSPIRE].

[20] CMS collaboration, *Search for soft unclustered energy patterns produced in association with a W or Z boson in proton-proton collisions at* $\sqrt{s} = 13$ *TeV*, *Phys. Lett. B* **879** (2026) 140671 [arXiv:2604.05996] [INSPIRE].

[21] Y. Hatta and T. Matsuo, *Thermal hadron spectrum in* e^+e^- *annihilation from gauge/string duality*, *Phys. Rev. Lett.* **102** (2009) 062001 [arXiv:0807.0098] [INSPIRE].

[22] R. Hagedorn, *Statistical thermodynamics of strong interactions at high-energies*, *Nuovo Cim. Suppl.* **3** (1965) 147 [INSPIRE].

[23] M. Graham, C. Hearty and M. Williams, *Searches for Dark Photons at Accelerators*, *Ann. Rev. Nucl. Part. Sci.* **71** (2021) 37 [arXiv:2104.10280] [INSPIRE].

[24] S. Knapen, J. Shelton and D. Xu, *Perturbative benchmark models for a dark shower search program*, *Phys. Rev. D* **103** (2021) 115013 [arXiv:2103.01238] [INSPIRE].

[25] ATLAS collaboration, *The ATLAS Experiment at the CERN Large Hadron Collider*, 2008 *JINST* **3** S08003 [INSPIRE].

[26] ATLAS Collaboration, *ATLAS Insertable B-Layer: Technical Design Report*, ATLAS-TDR-19.

[27] ATLAS IBL collaboration, *Production and Integration of the ATLAS Insertable B-Layer*, 2018 *JINST* **13** T05008 [arXiv:1803.00844] [INSPIRE].

[28] G. Avoni et al., *The new LUCID-2 detector for luminosity measurement and monitoring in ATLAS*, 2018 *JINST* **13** P07017 [INSPIRE].

[29] ATLAS collaboration, *Performance of the ATLAS Trigger System in 2015*, *Eur. Phys. J. C* **77** (2017) 317 [arXiv:1611.09661] [INSPIRE].

[30] ATLAS collaboration, *Software and computing for Run 3 of the ATLAS experiment at the LHC*, *Eur. Phys. J. C* **85** (2025) 234 [*Erratum ibid.* **85** (2025) 907] [arXiv:2404.06335] [INSPIRE].

[31] ATLAS collaboration, *ATLAS data quality operations and performance for 2015–2018 data-taking*, 2020 *JINST* **15** P04003 [arXiv:1911.04632] [INSPIRE].

[32] S. Mrenna and P. Skands, *Automated Parton-Shower Variations in Pythia 8*, *Phys. Rev. D* **94** (2016) 074005 [arXiv:1605.08352] [INSPIRE].

JHEP10(2026)206

[33] ATLAS collaboration, *ATLAS Pythia 8 tunes to 7 TeV data*, ATL-PHYS-PUB-2014-021 [INSPIRE].

[34] NNPDF collaboration, *Parton distributions for the LHC Run II*, *JHEP* **04** (2015) 040 [arXiv:1410.8849] [INSPIRE].

[35] LHC Higgs Cross Section Working Group collaboration, *Handbook of LHC Higgs Cross Sections: 4. Deciphering the Nature of the Higgs Sector*, arXiv:1610.07922 [DOI:10.23731/CYRM-2017-002] [INSPIRE].

[36] ATLAS collaboration, *The ATLAS Simulation Infrastructure*, *Eur. Phys. J. C* **70** (2010) 823 [arXiv:1005.4568] [INSPIRE].

[37] K. Hamilton, P. Nason, E. Re and G. Zanderighi, *NNLOPS simulation of Higgs boson production*, *JHEP* **10** (2013) 222 [arXiv:1309.0017] [INSPIRE].

[38] K. Hamilton, P. Nason and G. Zanderighi, *Finite quark-mass effects in the NNLOPS POWHEG+MiNLO Higgs generator*, *JHEP* **05** (2015) 140 [arXiv:1501.04637] [INSPIRE].

[39] S. Alioli, P. Nason, C. Oleari and E. Re, *A general framework for implementing NLO calculations in shower Monte Carlo programs: the POWHEG BOX*, *JHEP* **06** (2010) 043 [arXiv:1002.2581] [INSPIRE].

[40] P. Nason, *A new method for combining NLO QCD with shower Monte Carlo algorithms*, *JHEP* **11** (2004) 040 [hep-ph/0409146] [INSPIRE].

[41] S. Frixione, P. Nason and C. Oleari, *Matching NLO QCD computations with Parton Shower simulations: the POWHEG method*, *JHEP* **11** (2007) 070 [arXiv:0709.2092] [INSPIRE].

[42] S. Alioli, P. Nason, C. Oleari and E. Re, *NLO vector-boson production matched with shower in POWHEG*, *JHEP* **07** (2008) 060 [arXiv:0805.4802] [INSPIRE].

[43] T. Sjöstrand, S. Mrenna and P.Z. Skands, *A Brief Introduction to PYTHIA 8.1*, *Comput. Phys. Commun.* **178** (2008) 852 [arXiv:0710.3820] [INSPIRE].

[44] ATLAS collaboration, *Measurement of the Z/γ^* boson transverse momentum distribution in pp collisions at $\sqrt{s} = 7$ TeV with the ATLAS detector*, *JHEP* **09** (2014) 145 [arXiv:1406.3660] [INSPIRE].

[45] H.-L. Lai et al., *New parton distributions for collider physics*, *Phys. Rev. D* **82** (2010) 074024 [arXiv:1007.2241] [INSPIRE].

[46] J. Pumplin et al., *New generation of parton distributions with uncertainties from global QCD analysis*, *JHEP* **07** (2002) 012 [hep-ph/0201195] [INSPIRE].

[47] P. Golonka and Z. Was, *PHOTOS Monte Carlo: A precision tool for QED corrections in Z and W decays*, *Eur. Phys. J. C* **45** (2006) 97 [hep-ph/0506026] [INSPIRE].

[48] N. Davidson, T. Przedzinski and Z. Was, *PHOTOS interface in C++: Technical and Physics Documentation*, *Comput. Phys. Commun.* **199** (2016) 86 [arXiv:1011.0937] [INSPIRE].

[49] D.J. Lange, *The EvtGen particle decay simulation package*, *Nucl. Instrum. Meth. A* **462** (2001) 152 [INSPIRE].

[50] S. Frixione, P. Nason and G. Ridolfi, *A positive-weight next-to-leading-order Monte Carlo for heavy flavour hadroproduction*, *JHEP* **09** (2007) 126 [arXiv:0707.3088] [INSPIRE].

[51] ATLAS collaboration, *Studies on top-quark Monte Carlo modelling for Top2016*, ATL-PHYS-PUB-2016-020 (2016) [INSPIRE].

JHEP10(2026)206

[52] T. Sjöstrand et al., *An introduction to PYTHIA 8.2*, *Comput. Phys. Commun.* **191** (2015) 159 [arXiv:1410.3012] [INSPIRE].

[53] R.D. Ball et al., *Parton distributions with LHC data*, *Nucl. Phys. B* **867** (2013) 244 [arXiv:1207.1303] [INSPIRE].

[54] J. Alwall et al., *The automated computation of tree-level and next-to-leading order differential cross sections, and their matching to parton shower simulations*, *JHEP* **07** (2014) 079 [arXiv:1405.0301] [INSPIRE].

[55] SHERPA collaboration, *Event Generation with Sherpa 2.2*, *SciPost Phys.* **7** (2019) 034 [arXiv:1905.09127] [INSPIRE].

[56] T. Gleisberg and S. Hoeche, *Comix, a new matrix element generator*, *JHEP* **12** (2008) 039 [arXiv:0808.3674] [INSPIRE].

[57] S. Schumann and F. Krauss, *A parton shower algorithm based on Catani-Seymour dipole factorisation*, *JHEP* **03** (2008) 038 [arXiv:0709.1027] [INSPIRE].

[58] S. Hoeche, F. Krauss, M. Schönherr and F. Siegert, *A critical appraisal of NLO+PS matching methods*, *JHEP* **09** (2012) 049 [arXiv:1111.1220] [INSPIRE].

[59] S. Hoeche, F. Krauss, M. Schönherr and F. Siegert, *QCD matrix elements + parton showers: The NLO case*, *JHEP* **04** (2013) 027 [arXiv:1207.5030] [INSPIRE].

[60] S. Catani, F. Krauss, R. Kuhn and B.R. Webber, *QCD matrix elements + parton showers*, *JHEP* **11** (2001) 063 [hep-ph/0109231] [INSPIRE].

[61] S. Hoeche, F. Krauss, S. Schumann and F. Siegert, *QCD matrix elements and truncated showers*, *JHEP* **05** (2009) 053 [arXiv:0903.1219] [INSPIRE].

[62] F. Buccioni et al., *OpenLoops 2*, *Eur. Phys. J. C* **79** (2019) 866 [arXiv:1907.13071] [INSPIRE].

[63] F. Cascioli, P. Maierhöfer and S. Pozzorini, *Scattering Amplitudes with Open Loops*, *Phys. Rev. Lett.* **108** (2012) 111601 [arXiv:1111.5206] [INSPIRE].

[64] A. Denner, S. Dittmaier and L. Hofer, *COLLIER: a fortran-based Complex One-Loop LIbrary in Extended Regularizations*, *Comput. Phys. Commun.* **212** (2017) 220 [arXiv:1604.06792] [INSPIRE].

[65] ATLAS collaboration, *The Pythia 8 A3 tune description of ATLAS minimum bias and inelastic measurements incorporating the Donnachie-Landshoff diffractive model*, ATL-PHYS-PUB-2016-017 (2016) [INSPIRE].

[66] ATLAS collaboration, *Performance of the ATLAS muon triggers in Run 2*, 2020 *JINST* **15** P09015 [arXiv:2004.13447] [INSPIRE].

[67] ATLAS collaboration, *Track and Vertex Reconstruction with the ATLAS Inner Detector*, arXiv:2605.07585 [INSPIRE].

[68] ATLAS collaboration, *Muon reconstruction and identification efficiency in ATLAS using the full Run 2 pp collision data set at* $\sqrt{s} = 13$ *TeV*, *Eur. Phys. J. C* **81** (2021) 578 [arXiv:2012.00578] [INSPIRE].

[69] G. Hanson et al., *Evidence for Jet Structure in Hadron Production by* e^+e^- *Annihilation*, *Phys. Rev. Lett.* **35** (1975) 1609 [INSPIRE].

[70] ATLAS collaboration, *Reconstruction of primary vertices at the ATLAS experiment in Run 1 proton–proton collisions at the LHC*, *Eur. Phys. J. C* **77** (2017) 332 [arXiv:1611.10235] [INSPIRE].

JHEP10(2026)206

[71] ATLAS collaboration, *Luminosity determination in pp collisions at $\sqrt{s} = 13$ TeV using the ATLAS detector at the LHC*, *Eur. Phys. J. C* **83** (2023) 982 [arXiv:2212.09379] [INSPIRE].

[72] ATLAS collaboration, *Measurement of the Inelastic Proton-Proton Cross Section at $\sqrt{s} = 13$ TeV with the ATLAS Detector at the LHC*, *Phys. Rev. Lett.* **117** (2016) 182002 [arXiv:1606.02625] [INSPIRE].

[73] G. Cowan, K. Cranmer, E. Gross and O. Vitells, *Asymptotic formulae for likelihood-based tests of new physics*, *Eur. Phys. J. C* **71** (2011) 1554 [*Erratum ibid.* **73** (2013) 2501] [arXiv:1007.1727] [INSPIRE].

[74] A.L. Read, *Presentation of search results: The CL_s technique*, *J. Phys. G* **28** (2002) 2693 [INSPIRE].

[75] ATLAS collaboration, *Combination of searches for invisible decays of the Higgs boson using 139 fb^{-1} of proton-proton collision data at $\sqrt{s} = 13$ TeV collected with the ATLAS experiment*, *Phys. Lett. B* **842** (2023) 137963 [arXiv:2301.10731] [INSPIRE].

[76] ATLAS collaboration, *ATLAS Computing Acknowledgements*, ATL-SOFT-PUB-2026-001.

JHEP10(2026)206

The ATLAS collaboration

G. Aad[102], E. Aakvaag[17], B. Abbott[121], S. Abdelhameed[83b], K. Abeling[54], N.J. Abicht[48], S.H. Abidi[30], M. Aboelela[44], A. Aboulhorma[36e], H. Abramowicz[154], B.S. Acharya[68a,68b,a], A. Ackermann[62a], J. Ackerschott[55], C. Adam Bourdarios[4], L. Adamczyk[85a], S.V. Addepalli[146], M. J. Addison[101], J. Adelman[117], A. Adiguzel[22c], T. Adye[135], A.A. Affolder[137], Y. Afik[39], M.N. Agaras[13], A. Aggarwal[100], C. Agheorghiesei[28c], A. Ahmad[83a], F. Ahmadov[38,b], S. Ahuja[165], X. Ai[113c], G. Aielli[75a,75b], A. Aikot[165], M. Ait Tamlihat[36e], T.P.A. Åkesson[98], D. Akiyama[170], N.N. Akolkar[25], S. Aktas[168], G.L. Alberghi[24b], J. Albert[167], U. Alberti[20], P. Albicocco[52], S. Alderweireldt[51], Z.L. Alegria[122], M. Aleksa[37], I.N. Aleksandrov[38], C. Alexa[28b], T. Alexopoulos[10], F. Alfonsi[24b], M. Algren[55], M. Alhroob[169], B. Ali[133], H. M. J. Ali[91,c], S. Ali[32], S.W. Alibocus[92], M. Aliev[34c], G. Alimonti[70a], C. Allaire[65], B.M.M. Allbrooke[149], D. R. Allen[122], J. S. Allen[101], J.F. Allen[51], C.S. Alley[1], E.R. Almazan[137], A. Aloisio[71a,71b], F. Alonso[90], C. Alpigiani[140], A. Alvarez Fernandez[100], M. Alves Cardoso[55], M.G. Alviggi[71a,71b], Y. Amaral Coutinho[81b], C. Amelung[37], M. Amerl[101], T. Amezza[128], B. Amini[53], K. Amirie[158], A. Amirkhanov[38], D. Amperiadou[155], C. Anastopoulos[142], T. Andeen[11], J.K. Anders[92], A. C. Anderson[58], A. Andreazza[70a,70b], S. Angelidakis[9], A. Angerami[41], A.V. Anisenkov[38], A. Annovi[73a], C. Antel[37], E. Antipov[148], M. Antonelli[52], F. Anulli[74a], M. Aoki[82], T. Aoki[156], M.A. Aparo[13], L. Aperio Bella[47], M. Apicella[31], C. Appelt[154], A. Apyan[27], R. Arakida[125], M. Arampatzi[10], S. J. Arbiol Val[86], C. Arcangeletti[52], A.T.H. Arce[50], M. Arcuri[43b,43a], J-F. Arguin[108], S. Argyropoulos[155], J.-H. Arling[47], O. Arnaez[4], H. Arnold[148], G. Artoni[74a,74b], H. Asada[111], S. Asatryan[175], N.A. Asbah[37], R. A. Ashby Pickering[169], A. M. Aslam[95], J. Assahsah[36d], K. Assamagan[30], R. Astalos[29a], K. S. V. Astrand[98], S. Atashi[162], R.J. Atkin[34a], H. Atmani[36f], P.A. Atmasiddha[129], K. Augsten[133], A.D. Auriol[40], V.A. Austrup[101], A.S. Avad[94], G. Avolio[37], A. Azzam[13], D. Babal[29b], H. Bachacou[136], K. Bachas[155,d], A. Bachiu[35], E. Bachmann[49], M. J. Backes[62a], A. Badea[39], T.M. Baer[106], M. Bahmani[19], D. Bahner[53], K. Bai[124], L. Baines[94], O.K. Baker[174], D. Bakshi Gupta[8], L.E. Balabram Filho[81b], V. Balakrishnan[121], R. Balasubramanian[4], P. Balek[85a], E. Ballabene[24b,24a], F. Balli[136], L.M. Baltes[62a], W.K. Balunas[127], I. Bamwidhi[83c], E. Banas[86], M. Bandieramonte[130], S. Bansal[25], L. Barak[154], M. Barakat[47], E.L. Barberio[105], D. Barberis[18b], M. Barbero[102], M. Z. Barel[116], T. Barillari[110], M-S. Barisits[37], T. Barklow[146], P. Baron[134], D.A. Baron Moreno[101], A. Baroncelli[61], A.J. Barr[127,e], J.D. Barr[96], F. Barreiro[99], J. Barreiro Guimarães da Costa[14], M.G. Barros Teixeira[131a], F. Bartels[37], R. Bartoldus[146], A.E. Barton[91], P. Bartos[29a], M. Baselga[48], S. Bashiri[86], A. Bassalat[65,f], M.J. Basso[159a], S. Bataju[44], R. Bate[166], R.L. Bates[58], M. Battaglia[137], D. Battulga[19], M. Bauce[74a,74b], L. Bauckhage[47], P. Bauer[25], L. T. Bayer[47], L.T. Bazzano Hurrell[31], T. Beau[128], J.Y. Beaucamp[90], S. Beauceron[128], P.H. Beauchemin[161], P. Bechtle[25], H.P. Beck[20,g], K. Becker[169], A.J. Beddall[80], V.A. Bednyakov[38], C.P. Bee[148], L.J. Beemster[16], M. Begalli[81d], M. Begel[30], J.K. Behr[47], J.F. Beirer[37], F. Beisiegel[25], I.B. Belean[28d], M. Belfkir[83c], G. Bella[154], L. Bellagamba[24b], A. Bellerive[35], C.D. Bellgraph[67], P. Bellos[21], I. Benaoumeur[21], D. Benchekroun[36a], F. Bendebba[36a], Y. Benhammou[154],

JHEP10(2026)206

K.C. Benkendorfer[167], L. Beresford[47], M. Beretta[52], E. Bergeaas Kuutmann[163], N. Berger[4], B. Bergmann[133], J. Beringer[18a], M. Berkat[136], G. Bernardi[5], C. Bernius[146], F.U. Bernlochner[25], A. Berrocal Guardia[13], T. Berry[95], P. Berta[134], A. Berti[131a], R. Bertrand[102], S. Bethke[110], A. Betti[74a,74b], T.F. Beumker[173], A.J. Bevan[94], L. Bezio[55], N.K. Bhalla[53], S. Bharthuar[110], S. Bhatta[148], P. Bhattarai[146], Z.M. Bhatti[118], K. D. Bhide[164], V.S. Bhopatkar[122], R.M. Bianchi[130], G. Bianco[24b,24a], O. Biebel[109], M. Biglietti[76a], P. Bijl[53], C. S. Billingsley[44], Y. Bimgdi[36f], M. Bindi[54], A. Bingham[173], A. Bingul[22b], C. Bini[74a,74b], M. Biros[134], S. Biryukov[149], T. Bisanz[48], E. Bisceglie[24b,24a], J.P. Biswal[135], D. Biswas[144], M. Biyabi[14], I. Bloch[47], A. Blue[58], U. Blumenschein[94], V.S. Bobrovnikov[38], L. Boccardo[56b,56a], M. Boehler[53], D. Bogavac[13], L. S. Boggia[128], V. Boisvert[95], P. Bokan[163], T. Bold[85a], M. Bomben[5], M. Bona[94], M. Boonekamp[136], A.G. Borbély[58], G. Borissov[91], A. Borkar[168], D. Bortoletto[127], M. Borysova[171], D. Boscherini[24b], M. Bosman[13], K. Bouaouda[36a], L. Boudet[136], J. Boudreau[130], E.V. Bouhova-Thacker[91], D. Boumediene[40], R. Bouquet[56b,56a], A. Boveia[120], D. Boye[30], I.R. Boyko[38], L. Bozianu[55], J. Bracinik[21], N. Brahimi[4], G. Brandt[173], O. Brandt[33], B. Brau[103], R. Brener[171], L. Brenner[116], R. Brenner[163], S. Bressler[171], M. Brettell[96], G. Brianti[116], D. Britton[58], D. Britzger[110], I. Brock[25], R. Brock[107], H. Bronson[129], G. Brooijmans[41], A.J. Brooks[67], E. M. Brooks[159b], E. Brost[30], L.M. Brown[167,159a], L.E. Bruce[60], T.L. Bruckler[127], P.A. Bruckman de Renstrom[86], B. Brüers[47], A. Bruni[24b], G. Bruni[24b], D. Brunner[46a,46b], M. Bruschi[24b], N. Bruscino[74a,74b], T. Buanes[17], Q. Buat[140], D. Buchin[110], A.G. Buckley[58], J. Bucko[134], M. Buhring[49], O. Bulekov[80], B.A. Bullard[146], T. O. Buratovich[90], S. Burdin[92], C.D. Burgard[48], A.M. Burger[89], B. Burghgrave[8], O. Burlayenko[53], J. Burleson[164], J.C. Burzynski[121], V. Büscher[100], P.J. Bussey[58], O. But[25], J.M. Butler[26], C.M. Buttar[58], J.M. Butterworth[96], P. Butti[37], W. Buttinger[135], C.J. Buxo Vazquez[107], A.R. Buzykaev[38], S. Cabrera Urbán[165], L. Cadamuro[65], H. Cai[37], Y. Cai[24b,112c,24a], Y. Cai[112a], M.A. Cairo[129], V.M.M. Cairo[37], O. Cakir[3a], N. Calace[37], P. Calafiura[18a], G. Calderini[128], P. Calfayan[35], L. Calic[98], G. Callea[58], L.P. Caloba[81b], D. Calvet[40], S. Calvet[40], R. Camacho Toro[128], S. Camarda[37], D. Camarero Munoz[27], P. Camarri[75a,75b], C. Camincher[37], M. Campanelli[96], A. Camplani[42], V. Canale[71a,71b], A.C. Canbay[3a], E. Canonero[95], J. Cantero[165], F. Capocasa[27], P. Cappelli[27], M. Capua[43b,43a], A. Carbone[70a,70b], R. Cardarelli[75a], J.C.J. Cardenas[8], M. P. Cardiff[27], G. Carducci[43b,43a], T. Carli[37], G. Carlino[71a], J.I. Carlotto[13], B.T. Carlson[130,h], E.M. Carlson[167], L. Carminati[70a,70b], A. Carnelli[4], M. Carnesale[37], S. Caron[115], E. Carquin[138g], I.B. Carr[105], S. Carrà[72a,72b], G. Carratta[24b,24a], C. Carrion Martinez[165], A.M. Carroll[124], N. Cartalade[40], M.P. Casado[13,i], A. Casali[58], P. Casolaro[71a,71b], M. Caspar[47], F. Cassinese[90], F. Castiglioni[73a,73b], W.R. Castiglioni[39], F.L. Castillo[4], V. Castillo Gimenez[165], N.F. Castro[131a,131e], A. Catinaccio[37], J.R. Catmore[126], T. Cavaliere[4], V. Cavaliere[30], E. Celebi[80], S. Cella[30], V. Cepaitis[55], K. Cerny[123], A.S. Cerqueira[81a], A. Cerri[73a,j], L. Cerrito[75a,75b], F. Cerutti[18a], B. Cervato[70a,70b], A. Cervelli[24b], G. Cesarini[52], S.A. Cetin[80], V. C. Chabalala[34j], P.M. Chabrillat[128], R. Chakkappai[65], S. Chakraborty[169], A. Chambers[60], J. Chan[18a], J.D. Chapman[33], E. Chapon[136], D.G. Charlton[21], C. Chauhan[132], Y. Che[112a], S. Chekanov[6], G.A. Chelkov[38,k], H. Chen[30], J. Chen[141a],

JHEP10(2026)206

J. Chen[145], M. Chen[59], S. Chen[87], S.J. Chen[112a], X. Chen[141a], X. Chen[15,l], Z. Chen[61], C.L. Cheng[146], H.C. Cheng[63a], S. Cheong[146], A. Cheplakov[38], E. Cherepanova[116], E. Cheu[7], K. Cheung[64], L. Chevalier[136], G. Chiarelli[73a], G. Chiodini[69a], A.S. Chisholm[21], J. L. Chisholm[166], A. Chitan[28b], M. Chitishvili[165], M.V. Chizhov[38,m], K. Chmiel[76a,76b], K. Choi[11], Y. Chou[140], E.Y.S. Chow[115], G. Christou[51], K.L. Chu[171], M.C. Chu[63a], Z. Chubinidze[52], J. Chudoba[132], J.J. Chwastowski[86], D. Cieri[110], K.M. Ciesla[85a], V. Cindro[93], A. Ciocio[18a], F. Cirotto[71a,71b], Z.H. Citron[171], M. Citterio[70a], D.A. Ciubotaru[28b], A. Clark[55], P.J. Clark[51], N. Clarke Hall[37], C. Clarry[158], S.E. Clawson[37], C. Clement[46a,46b], L. Clissa[24b,24a], Y. Coadou[102], M. Cobal[68a,68c], A. Coccaro[56b], M. G. Cochran Branson[140], R.F. Coelho Barrue[131a], R. Coelho Lopes De Sa[103], S. Coelli[70a], M.M. Cohen[129], L. S. Colangeli[158], B. Cole[41], P. Collado Soto[99], J. Collot[59], M.R. Coluccia[69a], I. Combes[65], P. Conde Muiño[131a,131g], L.H.J. Condren[162], M.P. Connell[34c], S.H. Connell[34c], E.I. Conroy[161], M. Contreras Cossio[11], F. Conventi[71a,n], A.M. Cooper-Sarkar[127], L. Corazzina[74a,74b], F. A. Corchia[24b,24a], A. Cordeiro Oudot Choi[140], L.D. Corpe[40], M. Corradi[74a,74b], F. Corriveau[104,o], A. Cortes-Gonzalez[156], M.J. Costa[165], F. Costanza[4], D. Costanzo[142], J. Couthures[4], G. Cowan[95], K. Cranmer[172], L. Cremer[48], D. Cremonini[24b,24a], S. Crépé-Renaudin[59], F. Crescioli[128], T. Cresta[72a,72b], M. Cristinziani[144], M. Cristoforetti[77a,77b], T. M. Critchley[55], E. Critelli[96], A. Cueto[99], H. Cui[96], Z. Cui[7], B.M. Cunnett[149], W.R. Cunningham[58], E. Cuppini[110], F. Curcio[165], J. R. Curran[51], G. D'amen[30], V. D'Amico[109], M. D'Andrea[56b,56a], G. D'anniballe[73a,73b], S. D'Auria[70a,70b], A. D'Avanzo[71a,71b], L. D'Eramo[40], A. D'Onofrio[71a,71b], M. D'Onofrio[92], M. D'uffizi[101], M.J. Da Cunha Sargedas De Sousa[56b,56a], J.V. Da Fonseca Pinto[81b], C. Da Via[101], W. Dabrowski[85a], T. Dado[37], S. Dahbi[151], T. Dai[106], D. Dal Santo[20], C. Dallapiccola[103], M. Dam[42], J.R. Dandoy[35], D. Dannheim[37], M. Danninger[145], V. Dao[148], G. Darbo[56b], F. Dattola[47], T. Davidek[134], J. Davidson[169], I. Dawson[94], K. De[8], C. De Almeida Rossi[158], N. De Biase[47], S. De Castro[24b,24a], N. De Groot[115], P. de Jong[116], H. De la Torre[117], A. De Maria[112a], S. De Miranda Rimes[81d], A. De Salvo[74a], U. De Sanctis[75a,75b], F. De Santis[69a,69b], A. De Santo[149], J.B. De Vivie De Regie[59], K.G. De Vries[116], J. Debevc[93], D.V. Dedovich[38], J. Degens[92], A.M. Deiana[44], J. Del Peso[99], L. Delagrange[27], F. Deliot[136], C.M. Delitzsch[48], A. Dell'Acqua[37], L. Dell'Asta[70a,70b], M. Della Pietra[71a,71b], D. Della Volpe[55], M. Delmastro[4], C.C. Delogu[56b,56a], P.A. Delsart[59], S. Demers[174], M. Demichev[38], H. Denizli[22a,p], M.G. Depala[92], D. Derendarz[86], L. Derin[56b,56a], F. Derue[128], P. Dervan[92,†], A. M. Desai[1], K. Desch[25], F.A. Di Bello[73a,73b], A. Di Ciaccio[75a,75b], L. Di Ciaccio[4], D. Di Croce[37], C. Di Donato[71a,71b], A. Di Girolamo[37], G. Di Gregorio[65], A. Di Luca[77a,77b], B. Di Micco[76a,76b], R. Di Nardo[76a,76b], K.F. Di Petrillo[39], M. Diamantopoulou[154], F.A. Dias[116], M.A. Diaz[138a,138b], A. R. Didenko[38], M. Didenko[165], S.D. Diefenbacher[18a], E.B. Diehl[106], S. Díez Cornell[47], C. Diez Pardos[144], C. Dimitriadi[147], A. Dimitrievska[21], A. Dimri[148], Y. Ding[61], J. Dingfelder[25], T. Dingley[127], I-M. Dinu[28b], S.J. Dittmeier[62b], F. Dittus[37], M. Divisek[134], B. Dixit[92], F. Djama[102], T. Djobava[152b], C. Doglioni[101,98], A. Dohnalova[29a], Z. Dolezal[134], K. Domijan[85a], K.M. Dona[39], M. Donadelli[81d], B. Dong[107], J. Donini[40], J. Dopke[135], A. Doria[71a], N. Dos Santos Fernandes[131a],

JHEP10(2026)206

I.A. Dos Santos Luz[81e], P. Dougan[44], M.T. Dova[90], A.T. Doyle[58], M.P. Drescher[54], E. Dreyer[171], I. Drivas-koulouris[10], M. Drnevich[118], D. Du[61], T. Du[39], T.A. du Pree[116], Z. Duan[112a], M. Dubau[4], F. Dubinin[38], M. Dubovsky[29a], E. Duchovni[171], G. Duckeck[109], P. K. Duckett[96], O.A. Ducu[28b], D. Duda[51], A. Dudarev[37], M.M. Dudek[86], E. R. Duden[27], L. Duflot[65], M. Dührssen[37], I. Duminica[28g], A.E. Dumitriu[28b], M. Dunford[62a], T. Duong[4], A. Duperrin[102], A.F. Duque Bran[40], H. Duran Yildiz[3a], A. Durglishvili[152b], G.I. Dyckes[18a], M. Dyndal[85a], B.S. Dziedzic[37], G.H. Eberwein[127], B. Eckerova[29a], J.C. Egan[96], S. Eggebrecht[54], E. Egidio Purcino De Souza[81e], G. Eigen[17], K. Einsweiler[18a], T. Ekelof[163], P.A. Ekman[98], S. El Farkh[36b], Y. El Ghazali[61], H. El Jarrari[104], A. El Moussaouy[36a], I. Elbaz[154], D. Elitez[37], M. Ellert[163], F. Ellinghaus[173], T.A. Elliot[95], J. Elmsheuser[30], M. Elsawy[83b], M. Elsing[37], D. Emeliyanov[135], Y. Enari[82], S. Epari[108], D. Ernani Martins Neto[86], F. Ernst[37], M. Escalier[65], C. Escobar[165], R. Estevam De Paula[81c], E. Etzion[154], G. Evans[131a,131b], H. Evans[67], L.S. Evans[47], S. Ezzarqtouni[36a], F. Fabbri[24b,24a], L. Fabbri[24b,24a], G. Facini[96], V. Fadeyev[137], D. Fakoudis[100], S. Falciano[74a], L.F. Falda Ulhoa Coelho[27], F. Fallavollita[110], G. Falsetti[43b,43a], J. Faltova[134], C. Fan[164], K. Y. Fan[63b], Y. Fan[14], Y. Fang[14,112c], M. Fanti[70a,70b], M. Faraj[68a,68c], Z. Farazpay[97], A. Farbin[8], A. Farilla[76a], K. Farman[151], J. N. Farr[174], M. S. Farrington[60], S.M. Farrington[135,51], F. Fassi[36e], D. Fassouliotis[9], L. Fayard[65], G. Fazzino[62b], P. Federic[134], P. Federicova[132], M. Feickert[172], L. Feligioni[102], D.E. Fellers[18a], C. Feng[113b], Y. Feng[14], Z. Feng[65], B. Fernandez Barbadillo[91], P. Fernandez Martinez[66], C. Fernandez Ruiz[33], J. Ferrando[91], A. Ferrari[163], P. Ferrari[116,115], R. Ferrari[72a], D. Ferrere[55], C. Ferretti[106], M. P. Fewell[1], D. Fiacco[74a,74b], F. Fiedler[100], P. Fiedler[133], S. Filimonov[38], M.S. Filip[28b,q], A. Filipčič[93], M. Filipig[68a,68c], E.K. Filmer[159a], F. Filthaut[115], M.C.N. Fiolhais[131a,131c,r], L. Fiorini[165], W.C. Fisher[107], T. Fitschen[101], I. Fleck[144], P. Fleischmann[106], T. Flick[173], M. Flores[34d,s], L.R. Flores Castillo[63a], M. Foll[126], F.M. Follega[77a,77b], N. Fomin[33], A. Formica[136], M. Fornasiero[149], A.C. Forti[101], N. Forti[24b,24a], E. Fortin[102], A.W. Fortman[18a], L. Foster[18a], L. Fountas[9], H. Fox[91], P. Francavilla[73a,73b], S. Francescato[60], S. Franchellucci[20], M. Franchini[24b,24a], S. Franchino[62a], D. Francis[37], L. Franco[47], L. Franconi[47], M. Franklin[60], G. Frattari[37], Y.Y. Frid[154], N. Fritzsche[37], A. Froch[55], D. Froidevaux[37], J.A. Frost[135], Y. Fu[107], S. Fuenzalida Garrido[138g], Y.C. Fujikake[137], M. Fujimoto[148], K. Y. Fung[63a], E. Furtado De Simas Filho[81e], M. Furukawa[156], M. Fuste Costa[47], P. Fuste Martin[13], J. Fuster[165], A. Gaa[54], A. Gabrielli[24b,24a], A. Gabrielli[158], G. Gagliardi[56b,56a], L.G. Gagnon[146], S. Galantzan[154], J. Gallagher[1], E.J. Gallas[127], A.L. Gallen[163], B.J. Gallop[135], K.K. Gan[120], Y. Gao[51], Z. Gao[112a], A. Garabaglu[140], F.M. Garay Walls[138a,138b], C. García[165], A. Garcia Alonso[116], A.G. Garcia Caffaro[174], J.E. García Navarro[165], M. A. Garcia Ruiz[23b], M. Garcia-Sciveres[18a], G.L. Gardner[129], R.W. Gardner[39], N. Garelli[161], R.B. Garg[146], J.M. Gargan[33], C.A. Garner[158], C.M. Garvey[34a], V. K. Gassmann[161], G. Gaudio[72a], A.J. Gavin[94], J. Gavranovic[93], I.L. Gavrilenko[131a], C. Gay[166], G. Gaycken[124], A. Gekow[120], C. Gemme[56b], M.H. Genest[59], A. D. Gentry[114], S. George[95], T. Geralis[45], A. A. Gerwin[121], P. Gessinger-Befurt[37], M. Ghani[169], K. Ghorbanian[94], A. Ghosal[144], A. Ghosh[162], A. Ghosh[7], B. Giacobbe[24b], S. Giagu[74a,74b], A. Giannini[61], S.M. Gibson[95],

JHEP10(2026)206

D.T. Gil[85b], B.J. Gilbert[41], D. Gillberg[35], G. Gilles[116], D.M. Gingrich[2,t], M.P. Giordani[68a,68c], P.F. Giraud[136], G. Giugliarelli[68a,68c], D. Giugni[70a], F. Giuli[75a,75b,u], I. Gkialas[9,v], B.C. Gladwyn[127], C. Glasman[99], M. Glazewska[20], R. M. Gleason[162], G. Glemža[47], I. Gnesi[24b,24a,w], Y. Go[30], M. Goblirsch-Kolb[37], B. Gocke[48], D. Godin[108], B. Gokturk[22a], S. Goldfarb[105], T. Golling[55], M.G.D. Gololo[34c], A. Golub[140], J.P. Gombas[107], A. Gomes[131a,131b], G. Gomes Da Silva[144], A.J. Gomez Delegido[37], R. Gonçalo[131a], A. Gongadze[152c], F. Gonnella[21], J.L. Gonski[146], R.Y. González Andana[51], S. González de la Hoz[165], M. V. Gonzalez Rodrigues[47], R. Gonzalez Suarez[163], S. Gonzalez-Sevilla[55], L. Goossens[37], B. Gorini[37], E. Gorini[69a,69b], A. Gorišek[93], T.C. Gosart[129], A.T. Goshaw[50], M.I. Gostkin[38], S. Goswami[122], C.A. Gottardo[37], S. A. Gotz[109], M. Gouighri[36b], A.G. Goussiou[140], N. Govender[34c], R. P. Grabarczyk[127], I. Grabowska-Bold[85a], K. Graham[35], E. Gramstad[126], S. Grancagnolo[69a,69b], C.M. Grant[1], P.M. Gravila[28f], F.G. Gravili[69a,69b], H.M. Gray[18a], M. Greco[110], M. J. Green[1], C. Grefe[25], A. S. Grefsrud[37], I.M. Gregor[47], K.T. Greif[162], P. Grenier[146], S.G. Grewe[110], K. Grimm[32], S. Grinstein[13,x], E. Gross[171], J. Grosse-Knetter[54], L.H. Grossman[18b], L. Guan[106], W. Guérin[89], G. Guerrieri[37], R. Guevara[126], R. Gugel[100], J.A.M. Guhit[106], A. Guida[19], E. Guilloton[169], S. Guindon[37], F. Guo[14,112c], J. Guo[141a], L. Guo[47], L. Guo[112b,y], Y. Guo[106], Y. Guo[41], A. Gupta[48], R. Gupta[130], S. Gupta[27], S. Gurbuz[25], S.S. Gurdasani[47], G. Gustavino[74a,74b], P. Gutierrez[121], L.F. Gutierrez Zagazeta[129], M. Gutsche[49], C. Gutschow[96], C. Gwenlan[127], C.B. Gwilliam[92], E.S. Haaland[126], A. Haas[118], M. Habedank[58], C. Haber[18a], R.J. Haberle[171], H.K. Hadavand[8], A. Haddad[40], A. Hadef[49], K. E. Haeussler[53], A.I. Hagan[91], J. J. Hahn[144], M. Haleem[168], J. Haley[122], G.D. Hallewell[102], J.A. Hallford[47], H. Hamdaoui[163], M. Hamer[25], S. E. D. Hammoud[65], E.J. Hampshire[95], L. Han[112a], L. Han[61], S. Han[14], K. Hanagaki[82], M. Hance[137], D.A. Hangal[41], H. Hanif[145], M.D. Hank[129], J.B. Hansen[42], P.H. Hansen[42], T. Harenberg[173], S. Harkusha[175], M.L. Harris[103], Y.T. Harris[25], J. Harrison[13], P.F. Harrison[169], M. L. E. Hart[96], N.M. Hartman[110], N.M. Hartmann[109], R. Z. Hasan[95,135], Y. Hasegawa[143], D. Hashimoto[111], F. Haslbeck[37], S. Hassan[126], R. Hauser[107], M. Haviernik[134], C.M. Hawkes[21], R.J. Hawkings[37], Y. Hayashi[156], D. Hayden[107], R.L. Hayes[116], C.P. Hays[127], J.M. Hays[94], H.S. Hayward[92], M. He[14,112c], Y. He[47], Y. He[96], V. Hedberg[98], J. Heilman[35], S. Heim[47], T. Heim[18a], J.J. Heinrich[124], L. Heinrich[110], J. Hejbal[132], M. Helbig[49], A. Held[172], S. Hellesund[17], C.M. Helling[166], F.N.E. Henry[58], H. Herde[98], Y. Hernández Jiménez[148], G. Herten[53], R. Hertenberger[109], L. Hervas[37], M.E. Hesping[100], N.P. Hessey[159a], J. Hessler[110], R. Hicks[129], M. Hidaoui[36b], N. Hidic[134], E. Hill[158], T. S. Hillersoy[17], S.J. Hillier[21], J.R. Hinds[107], F. Hinterkeuser[25], M. Hirose[125], S. Hirose[170], D. Hirschbuehl[173], B. Hiti[93], J. Hobbs[148], R. Hobincu[28e], N. Hod[171], A.M. Hodges[164], M.C. Hodgkinson[142], B.H. Hodkinson[127], A. Hoecker[37], D. D. Hofer[106], J. Hofer[165], J. Hofner[100], M. Holzbock[37], L.B.A.H. Hommels[33], V. Homsak[127], J. J. Hong[67], T.M. Hong[130], R. Honscheid[127], B.H. Hooberman[164], W.H. Hopkins[6], M. C. Hoppesch[164], Y. Horii[111], M. E. Horstmann[110], M.M. Horzela[54], S. Hou[151], M. R. Housenga[164], J. Howarth[58], J. Hoya[6], M. Hrabovsky[123], T. Hryn'ova[4], P.J. Hsu[64], S.-C. Hsu[140], T. Hsu[65], M. Hu[18a], P. Hu[63b], Q. Hu[61], S. Huang[33], X. Huang[14,112c],

JHEP10(2026)206

Y. Huang[134], Y. Huang[112b], Y. Huang[14], Z. Huang[65], Z. Hubacek[133], F. Huegging[25], T.B. Huffman[127], M. Hufnagel Maranha De Faria[81a], C. A. Hugli[47], M. Huhtinen[37], S.K. Huiberts[17], R. Hulsken[104], C. E. Hultquist[18a], D.L. Humphreys[103], N. Huseynov[12], J. Huston[107], B. Huth[37], J. Huth[60], L. Huth[47], R. Hyneman[7], G. Iacobucci[55], G. Iakovidis[30], L. Iconomidou-Fayard[65], J. P. Iddon[37], P. Iengo[71a,71b], Y. Iiyama[156], T. Iizawa[156], Y. Ikegami[82], D. Iliadis[155], N. Ilic[158], H. Imam[36a], G. Inacio Goncalves[81d], S. A. Infante Cabanas[138c], T. Ingebretsen Carlson[46a,46b], J. M. Inglis[94], G. Introzzi[72a,72b], M. Iodice[76a], V. Ippolito[74a,74b], R. K. Irwin[92], M. Ishino[156], W. Islam[172], C. Issever[19], O. N. Istaitia[65,f], S. Istin[22a,z], K. Itabashi[125], H. Ito[170], R. Iuppa[77a,77b], A. Ivina[171], F. Ivone[37], S. Izumiyama[111], V. Izzo[71a], P. Jacka[133], P. Jackson[1], P. R. Jacobson[50], P. Jain[47], K. Jakobs[53], J. Jamieson[58], W. Jang[156], S. Jankovych[116], B. K. Jashal[135], M. Javurkova[103], P. Jawahar[101], L. Jeanty[124], J. Jejelava[152a,aa], P. Jenni[53,ab], L. Jerala[93], C.E. Jessiman[35], H. Jia[166], J. Jia[148], K. Jia[146], X. Jia[110,112c], C. Jiang[51], Q. Jiang[63b], S. Jiggins[47], M. Jimenez Ortega[165], J. Jimenez Pena[13], S. Jin[112a], A. Jinaru[28b], O. Jinnouchi[139], P. Johansson[142], K.A. Johns[7], J.W. Johnson[137], F. A. Jolly[47], D.M. Jones[149], E. Jones[47], P. Jones[33], R.W.L. Jones[91], T.J. Jones[92], H.L. Joos[37], R. Joshi[120], J. Jovicevic[16], X. Ju[18a], J.J. Junggeburth[37], T. Junkermann[62a], A. Juste Rozas[13,x], M.K. Juzek[86], S. Kabana[138f], A. Kaczmarska[86], S. A. Kadir[146], M. Kado[110], H. Kagan[120], M. Kagan[146], A. Kahn[129], C. Kahra[100], T. Kaji[156], E. Kajomovitz[153], N. Kakati[171], N. Kakoty[13], S. Kandel[8], E. Kanellaki[45], N. Kanellos[10], S. Kang[50], D. Kar[34j,†], E. Karentzos[25], K. Karki[8], O. Karkout[116], S.N. Karpov[38], Z.M. Karpova[38], V. Kartvelishvili[91,152b], E. Kasimi[155], J. Katzy[47], S. Kaur[35], R. Kavak[37], K. Kawade[143], M.P. Kawale[121], C. Kawamoto[87], E.F. Kay[37], S. Kazakos[107], K. Kazakova[102], J.M. Keaveney[34a], R. Keeler[167], G.V. Kehris[60], J.S. Keller[35], J. M. Kelly[167], J.I. Kelsey[164], J.J. Kempster[149], O. Kepka[132], J. Kerr[159b], B.P. Kerridge[135], B.P. Kerševan[93], L. Keszeghova[29a], M.B. Khan[93], R. A. Khan[130], A. Khanov[122], M. Kholodenko[131a], T.J. Khoo[19], G. Khoriauli[168], Y. Khoulaki[36a], Y.A.R. Khwaira[128], D. Kim[6], D.W. Kim[18b], Y.K. Kim[39], N. Kimura[96], M.K. Kingston[54], F. Kirfel[25], J. Kirk[135], A.E. Kiryunin[110], S. Kita[156], O. Kivernyk[25], M. Klassen[37], C. Klein[35], L. Klein[168], M.H. Klein[44], U. Klein[92], A. Klimentov[30], P. Kluit[116], S. Kluth[110], E. Kneringer[78], T.M. Knight[158], A. Knue[48], M. Kobel[49], D. Kobylianskii[171], S.F. Koch[37], M. Kocian[146], P. Kodyš[134], D.M. Koeck[124], T. Koffas[35], K. Kojima[82], O. Kolay[49], I. Koletsou[4], T. Komarek[86], S. Kondo[156], K. Köneke[54], A.X.Y. Kong[1], T. Kono[119], N. Konstantinidis[96], P. Kontaxakis[55], B. Konya[98], R. Kopeliansky[41], S. Koperny[85a], R. Koppenhofer[53], I. Kopsalis[10], K. Korcyl[86], K. Kordas[155,ac], A. Korn[96], S. Korn[54], I. Korolkov[13], O. Kortner[110], S. Kortner[110], W.H. Kostecka[117], M. Kostov[29a], V.V. Kostyukhin[144], A. Kotsokechagia[37], A. Kotwal[50], A. Koulouris[37], A. Kourkoumeli-Charalampidi[72a,72b], O. Kovanda[124], R. Kowalewski[167], W. Kozanecki[124], G. Kramberger[93], P. Kramer[25], A. Krasznahorkay[103], A. C. Kraus[117], J.W. Kraus[173], J.A. Kremer[47], N. B. Krengel[144], T. Kresse[158], L. Kretschmann[173], J. Kretzschmar[92], P. Krieger[158], K. Krizka[21], K. Kroeninger[48], H. Kroha[110], J. Kroll[132], J. Kroll[129], K.S. Krowpman[107], U. Kruchonak[38], H. Krüger[25], N. Krumnack[79], J. Krupa[146], M.C. Kruse[50], O. Kuchinskaia[38], S. Kuday[3a], S. Kuehn[37], R. Kuesters[53],

JHEP10(2026)206

T. Kuhl[47], V. Kukhtin[38], Y. Kulchitsky[38], S. Kuleshov[138d,138b], J. Kull[1], E. V. Kumar[109], M. Kumar[34j], N. Kumari[47], P. Kumari[159b], A. Kupco[132], O. Kuprash[53], H. Kurashige[84], L.L. Kurchaninov[159a], O. Kurdysh[4], M. Kuze[139], A.K. Kvam[103], J. Kvita[123], N.G. Kyriacou[140], M. Laassiri[30], C. Lacasta[165], H. Lacker[19], D. Lacour[128], E. Ladygin[38], A. Lafarge[40], B. Laforge[128], T. Lagouri[174], F.Z. Lahbabi[36a], S. Lai[54], W. S. Lai[96], I.K. Lakomiec[54], J.E. Lambert[167], S. Lammers[67], W. Lampl[7], C. Lampoudis[155], G. Lamprinoudis[168], A.N. Lancaster[117], U. Landgraf[53], M.P.J. Landon[94], V.S. Lang[53], A.J. Lankford[162], F. Lanni[37], C. S. Lantz[164], K. Lantzsch[25], A. Lanza[72a], M. Lanzac Berrocal[165], T. Lari[70a], D. Larsen[17], L. Larson[11], F. Lasagni Manghi[24b], M. Lassnig[37], H.C. Lau[167], S.D. Lawlor[142], R. Lazaridou[162], M. Lazzaroni[70a,70b], E. T. T. Le[162], H. D. M. Le[107], E.M. Le Boulicaut[174], D.O. Le Guennec[136], L.T. Le Pottier[18a], B. Leban[24b,24a], F. Ledroit-Guillon[59], T.F. Lee[159b], L.L. Leeuw[34h], M. Lefebvre[167], C. Leggett[18a], L.M. Lehmann[116], W.A. Leight[103], W. Leinonen[115], A. Leisos[155,ad], M.A.L. Leite[81c], C.E. Leitgeb[19], R. Leitner[134], E. Lelak[134], K.J.C. Leney[44], T. Lenz[25], S. Leone[73a], C. Leonidopoulos[51], A. Leopold[147], J. LePage-Bourbonnais[35], R. Les[65], C.G. Lester[33], J. Levêque[4], L.J. Levinson[171], G. Levrini[24b,24a], M.P. Lewicki[86], C. Lewis[140], D.J. Lewis[4], L. Lewitt[142], A. Li[30], B. Li[113b], C-Q. Li[110], C. Li[106], H. Li[113b], H. Li[101], H. Li[15], H. Li[61], H. Li[113b], J. Li[141a], L. Li[141a], R. Li[174], S. Li[141b,141a], Y. Li[14], Z. Li[14,112c], Z. Li[61], S. Liang[14,112c], Z. Liang[14], M. Liberatore[136], B. Liberti[75a], G. B. Libotte[81d], K. Lie[63c], J. Lieber Marin[81e], H. Lien[67], H. Lin[106], S. F. Lin[148], L. Linden[109], R.E. Lindley[7], J.H. Lindon[37], J. Ling[60], E. Lipeles[129], A. Lipniacka[17], A. Lister[166], J.D. Little[67], B. Liu[113a], B.X. Liu[112b], D. Liu[153], D. Liu[137], E. H. L. Liu[21], H. Liu[112b], J.K.K. Liu[118], K. Liu[141b], K. Liu[141b], M. Liu[61], M.Y. Liu[61], P. Liu[113b], Q. Liu[146], S. Liu[148], X. Liu[113b], Y. Liu[112b,112c], Y. Liu[164], Y.L. Liu[113b], Y.W. Liu[61], Z. Liu[65,ae], S.L. Lloyd[94], E.M. Lobodzinska[47], P. Loch[7], E. Lodhi[158], K. Lohwasser[142], E. Loiacono[122], J. D. Lomas[21], I. Longarini[162], R. Longo[24b,24a,w], A. Lopez Solis[13], N.A. Lopez-canelas[7], N. Lorenzo Martinez[4], A.M. Lory[109], M. Losada[83b], G. Löschcke Centeno[4], X. Lou[14,112c], P.A. Love[91], H. Lu[14], M. Lu[65], S. Lu[129], Y.J. Lu[151], H.J. Lubatti[140], C. Luci[74a,74b], F.L. Lucio Alves[112a], J.A. Lue[124], F. Luehring[67], B. S. Lunday[129], O. Lundberg[147], J. Lunde[37], N.A. Luongo[6], M.S. Lutz[158], A.B. Lux[26], D. Lynn[30], R. Lysak[132], V. Lysenko[133], E. Lytken[98], V. Lyubushkin[38], T. Lyubushkina[38], M.M. Lyukova[148], H. Ma[30], K. Ma[61], L.L. Ma[113b], W. Ma[61], Y. Ma[113b], B. Maček[93], P.C. Machado De Abreu Farias[81e], D. Macina[37], R. Madar[40], T. Madula[96], J. Maeda[84], S. Maeland[17], T. Maeno[30], P.T. Mafa[34f], G. Magni[65], H. Maguire[142], M. Maheshwari[33], V. Maiboroda[65], G. Maineri[70a,70b], A. Maio[131a,131b,131d], K. Maj[85a], O. Majersky[47], S. Majewski[124], A. Makita[156], N. Makovec[65], V. Maksimovic[16], B. Malaescu[128], J. Malamant[126], Pa. Malecki[86], F. Malek[59,af], M. Mali[93], D. Malito[95], A. Maloizel[5], A. Malvezzi Lopes[81d], S. Malyukov[38], J. Mamuzic[93], G. Mancini[52], M. N. Mancini[27], G. Manco[72a,72b], S.S. Mandarry[149], I. Mandić[93], L. Manhaes de Andrade Filho[81a], I.M. Maniatis[171], J. Manjarres Ramos[89], D.C. Mankad[171], A. Mann[109], T. Manoussos[100], M.N. Mantinan[39], S. Manzoni[37], L. Mao[141a], X. Mapekula[34c], A. Marantis[155], R.R. Marcelo Gregorio[1], G. Marchiori[5],

JHEP10(2026)206

C. Marcon[70a], E. Maricic[16], M. Marinescu[47], S. Marium[47], M. Marjanovic[121], A. Markhoos[53], M. Markovitch[65], M. K. Maroun[103], M. C. Marr[145], T. L. Marsault[136], G. T. Marsden[101], Z. Marshall[18a], S. Marti-Garcia[165], J. Martin[96], T.A. Martin[135], V.J. Martin[51], B. Martin dit Latour[17], S. Martin-Haugh[135], L. Martinelli[74a,74b], V.I. Martinez Outschoorn[103], P. Martinez Suarez[37], G. Martinovicova[134], V.S. Martoiu[28b], A. Martone[89], A.C. Martyniuk[96], A. Marzin[37], D. Mascione[77a,77b], L. Masetti[100], J. Masik[101], A.L. Maslennikov[38], S.L. Mason[41], P. Massarotti[71a,71b], P. Mastrandrea[73a,73b], A. Mastroberardino[43b,43a], R. Mastrofrancesco[72a,72b], T. Masubuchi[125], T.T. Mathew[124], J. Matousek[134], D.M. Mattern[48], K. Mauer[47], J. Maurer[28b], T. Maurin[58], C. Mavungu Tsava[102], A. E. May[101], E. Mayer[40], R. Mazini[34j], S.M. Mazza[137], E. Mazzeo[37], J.P. Mc Gowan[167], S.P. Mc Kee[106], C.C. McCracken[166], E.F. McDonald[105], L. F. Mcelhinney[91], J.A. Mcfayden[149], R.P. McGovern[167], R.P. Mckenzie[34j], D.J. Mclaughlin[96], S.J. McMahon[135], C.M. Mcpartland[92], R.A. McPherson[167,o], S. Mehlhase[109], A. Mehta[92], D. Melini[165], B.R. Mellado Garcia[14,ag], A.H. Melo[54], F. Meloni[47], A.M. Mendes Jacques Da Costa[101], L. Meng[91], S. Menke[110], M. Mentink[37], E. Meoni[43b,43a], G. Mercado[117], S. Merianos[155], C. Merlassino[68a,68c], C. Meroni[70a,70b], J. Metcalfe[6], A.S. Mete[6], E. Meuser[100], C. Meyer[67], J-P. Meyer[136], O. Mezhenska[29b], Y. Miao[112a], R.P. Middleton[135], M. Mihovilovic[65], L. Mijović[51], G. Mikenberg[171], M. Mikestikova[132], M. Mikuž[93], H. Mildner[100], A. Milic[37], D.W. Miller[39], E. H. Miller[146], A. Milov[171], D.A. Milstead[46a,46b], T. Min[112a], I.A. Minashvili[152b], A.I. Mincer[118], B. Mindur[85a], M. Mineev[38], L.M. Mir[13], M. Miralles Lopez[58], M. Mironova[18a], M. Missio[40], A. Mitra[169], V.A. Mitsou[165], P.S. Miyagawa[94], R. Mizuhiki[84], T. Mkrtchyan[37], M. Mlinarevic[96], T. Mlinarevic[96], M. Mlynarikova[134], L. Mlynarska[85a], C. Mo[141a], H. Mobius[47], S. Mobius[20], M. H. Mohamed Farook[114], S. Mohapatra[41], M.F. Mohd Soberi[51], S. Mohiuddin[122], G. Mokgatitswane[34j], R. Mole[21], L. Moleri[171], U. Molinatti[127], M. E. Mollerach[31], L.G. Mollier[20], L. Monaco[37,58], B. Mondal[132], S. Mondal[134], K. Mönig[47], E. Monnier[102], L. Monsonis Romero[165], A. Montella[46a,46b], M. Montella[120], F. Montereali[76a,76b], F. Monticelli[90], S. Monzani[68a,68c], M.E.E. Moors[25], A. Morancho Tarda[42], N. Morange[65], M. Moreno Llácer[165], C. Moreno Martinez[55], J.M. Moreno Perez[23b], P. Morettini[56b], S. Morgenstern[62a], M. Morii[60], M. Morinaga[156], F. Morodei[74a,74b], P. Moschovakos[37], B. Moser[53], M. Mosidze[152b], T. Moskalets[44], P. Moskvitina[115], C.J. Mosomane[34b], J. Moss[32], T. Motta Quirino[81d], A. Moussa[36d], Y. Moyal[171,ah], H. Moyano Gomez[13], E.J.W. Moyse[103], T.G. Mroz[86], S. Muanza[102], M. Mucha[25], P. Mucha[96], J. Mueller[130], D. Muller[144], G.A. Mullier[163], A.J. Mullin[33], J.J. Mullin[50], A.C. Mullins[44], A.E. Mulski[60], D.P. Mungo[158], D. Munoz Perez[122], F.J. Munoz Sanchez[101], W.J. Murray[169,135], E. Musajan[61], M. Muškinja[93], C. Mwewa[47], A.J. Myers[8], G. Myers[106], M. Myska[133], B.P. Nachman[146], I.A. Nadas[28d], K. Nagai[127], K. Nagano[82], R. Nagasaka[156], J.L. Nagle[30,ai], E. Nagy[102], A.M. Nairz[37], T. Nakagawa[87], Y. Nakahama[82], K. Nakamura[82], A. Nandi[62b], H. Nanjo[125], E.A. Narayanan[44], V.A. Narendran[127], Y. Narukawa[156], L. Nasella[70a,70b], S. Nasri[83c], C. Nass[25], G. Navarro[23a], A. Nayaz[19], S. Nechaeva[24b,24a], F. Nechansky[132], A. Negri[72a,72b], M. Negrini[24b], C. Nellist[116], C. Nelson[104], K. Nelson[106], S. Nemecek[132], M. Nessi[37,e], M.S. Neubauer[164], J. Newell[92],

JHEP10(2026)206

P.R. Newman[21], Y.W.Y. Ng[164], B. Ngair[83b], H.D.N. Nguyen[108], J.D. Nichols[121], R. Nicolaidou[136], J. Nielsen[137], M. Niemeyer[54], J. Niermann[37], N. Nikiforou[37], I. Nikolic-Audit[128], P. Nilsson[30], G. Ninio[154], A. Nisati[74a], D. Nishimura[156], R. Nisius[110], N. Nitika[171], E.K. Nkadimeng[34b], T. Nobe[156], D. Noll[146], T. Nommensen[150], M.B. Norfolk[142], B.J. Norman[35], L.C. Nosler[18a], M. Noury[36a], J. Novak[93], T. Novak[93], P. Novotny[171], R. Novotny[133], L. Nozka[123], K. Ntekas[37], D. Ntounis[146], N.M.J. Nunes De Moura Junior[81b], A.P. O'Neill[20], J. Ocariz[128], I. Ochoa[131a], A. Odella Rodriguez[13], S. Oerdek[47], J.T. Offermann[39], A. Ogrodnik[86], A. Oh[101], C.C. Ohm[147], H. Oide[82], M.L. Ojeda[37], Y. Okumura[156], L.F. Oleiro Seabra[131a], I. Oleksiyuk[55], G. Oliveira Correa[13], D. Oliveira Damazio[30], J.L. Oliver[1], R. Omar[67], Y. Onoda[139], A. Onofre[131a,131e,aj], P.U.E. Onyisi[11], M.J. Oreglia[39], D. Orestano[76a,76b], R. Orlandini[76a,76b], R.S. Orr[158], L.M. Osojnak[41], Y. Osumi[111], G. Otero y Garzón[31], H. Otono[88], M. Ouchrif[36d], F. Ould-Saada[126], T. Ovsiannikova[140], M. Owen[58], R.E. Owen[135], S.A. Oyeniran[114], V.E. Ozcan[22a], F. Ozturk[86], N. Ozturk[8], S. Ozturk[80], H.A. Pacey[127], K. Pachal[159a], A. Pacheco Pages[13], C. Padilla Aranda[13], G. Padovano[74a,74b], S. Pagan Griso[18a], L. Pagani[75a,75b], J. Pampel[25], D.K. Panchal[11], C.E. Pandini[59], J.G. Panduro Vazquez[135], H.D. Pandya[1], H. Pang[136], P. Pani[47], G. Panizzo[68a,68c], L. Panwar[128,ak], L. Paolozzi[21], S. Parajuli[164], A. Paramonov[6], C. Paraskevopoulos[52], D. Paredes Hernandez[63b], S.R. Paredes Saenz[51], A. Pareti[72a,72b], K.R. Park[41], T.H. Park[110], F. Parodi[56b,56a], J.A. Parsons[41], J.A. Partridge[137], U. Parzefall[53], B.A. Paschen[18a], B. Pascual Dias[40], L. Pascual Dominguez[99], E. Pasqualucci[74a], S. Passaggio[56b], F. Pastore[95], P. Patel[86], U.M. Patel[50], J.R. Pater[101], T. Pauly[37], A. Paunovic[16], F. Pauwels[134], C.I. Pazos[161], M. Pedersen[126], R. Pedro[131a], O. Penc[132], C.C. Penelaud[128], S. Peng[15], G. D. Penn[174], B.S. Peralva[81d], A.P. Pereira Peixoto[140], L. Pereira Sanchez[146], D.V. Perepelitsa[30,ai], G. Perera[103], E. Perez Codina[37], M. Perganti[10], H. Pernegger[37], S. Perrella[74a,74b], K. Peters[47], R.F.Y. Peters[101], B.A. Petersen[37], T.C. Petersen[42], E. Petit[102], V. Petousis[133], A. R. Petri[70a,70b], V.A. Petrovic[96], T. Petru[134], M. Pettee[18a], A. Petukhov[80], K. Petukhova[37], R. Pezoa[138g], L. Pezzotti[24b,24a], G. Pezzullo[174], L. Pfaffenbichler[37], A. J. Pfleger[78], T. Pham[105], T.M. Pham[172], P.W. Phillips[135], G. Piacquadio[148], E. Pianori[18a], F. Piazza[124], R. Piegaia[31], D. Pietreanu[28b], A.D. Pilkington[101], T. Pilusa[34j], M. Pinamonti[68a,68c], J.L. Pinfold[2], G. Pinheiro Matos[41], B.C. Pinheiro Pereira[131a], J. Pinol Bel[13], A. E. Pinto Pinoargote[128], L. Pintucci[68a,68c], K. M. Piper[149], A. Pirttikoski[55], D.A. Pizzi[35], L. Pizzimento[63b], A. Plebani[33], M.-A. Pleier[30], V. Pleskot[134], E. Plotnikova[38], G. Poddar[94], R. Poettgen[98], L. Poggioli[128], S. Polacek[134], G. Polesello[72a], A. Poley[145], A. Polini[24b], C.S. Pollard[169], Z.B. Pollock[120], E. Pompa Pacchi[121], N. I. Pond[96], D. Ponomarenko[67], L. Pontecorvo[37], S. Popa[28a], G.A. Popeneciu[28d], A. Poreba[37], D.M. Portillo Quintero[159a], S. Pospisil[133], M. A. Postill[142], P. Postolache[28c], K. Potamianos[169], P.A. Potepa[85a], I.N. Potrap[38], C.J. Potter[33], H. Potti[150], J. Poveda[165], M.E. Pozo Astigarraga[37], R. Pozzi[37], A. Prades Ibanez[75a,75b], S.R. Pradhan[142], J. Preston[95], J. Pretel[167], D. Price[101], M. Primavera[69a], L. Primomo[68a,68c], M.A. Principe Martin[99], R. Privara[123], T. Procter[85b], M.L. Proffitt[140], N. Proklova[129], K. Prokofiev[63c], G. Proto[110], J. Proudfoot[6],

JHEP10(2026)206

M. Przybycien[85a], W.W. Przygoda[85b], A. Psallidas[45], D. Pudzha[52], P. Puhl[57], H. I. Purnell[1], D. Pyatiizbyantseva[115], J. Qian[106], R. Qian[107], D. Qichen[127], Y. Qin[13], T. Qiu[51], A. Quadt[54], M. Queitsch-Maitland[101], G. Quetant[55], R.P. Quinn[166], D. Rafanoharana[110], J.L. Rainbolt[39], S. Rajagopalan[30], E. Ramakoti[38], L. Rambelli[56b,56a], I.A. Ramirez-Berend[35], K. Ran[106,112c], S. D. Randles[92], D. S. Rankin[129], N.P. Rapheeha[34j], H. Rasheed[28b], A. Rastogi[18a], S. Rave[100], S. Ravera[56b,56a], B. Ravina[37], I. Ravinovich[171], M. Raymond[37], A.L. Read[126], N.P. Readioff[142], D.M. Rebuzzi[72a,72b], A. S. Reed[58], K. Reeves[27], D. Reikher[37], T. Reisch[55], A. Rej[48], H. Ren[61], M. Renda[28b], F. Renner[47], A.G. Rennie[58], M. Repik[55], A.L. Rescia[43b,43a], S. Resconi[70a], M. Ressegotti[56b], S. Rettie[116], W.F. Rettie[35], M. M. Revering[33], O.L. Rezanova[38], P. Reznicek[134], H. Riani[36d], N. Ribaric[37], B. Ricci[68a,68c], E. Ricci[77a,77b], R. Richter[110], E. Richter-Was[85b], M. Ridel[128], S. Ridouani[36d], P. Riedler[37], E.M. Riefel[46a,46b], J. O. Rieger[116], M. Rimoldi[34c], L. Rinaldi[24b,24a], P. Rincke[163,54], G. Ripellino[163], I. Riu[13], J.C. Rivera Vergara[167], F. Rizatdinova[122], E. Rizvi[94], B.R. Roberts[39], S.S. Roberts[137], D. Robinson[33], A. Robson[58], A. Rocchi[75a,75b], C. Roda[73a,73b], F.A. Rodriguez[117], S. Rodriguez Bosca[37], Y. Rodriguez Garcia[23a], A.M. Rodríguez Vera[117], S. Roe[37], J.T. Roemer[37], O. Røhne[126], R.A. Rojas[37], Z. Rokavec[93], C.P.A. Roland[128], A. Romaniouk[78], E. Romano[72a,72b], M. Romano[24b], N. Rompotis[92], L. Roos[128], S. Rosati[74a], L. Roscher[47], B.J. Rosser[39], E. Rossi[127], E. Rossi[71a,71b], L.P. Rossi[60], L. Rossini[53], R. Rosten[120], M. Rotaru[28b], R. Roth[37], F. A. Rothen[55], D. Rousseau[65], D. Rousso[47], S. Roy-Garand[55], A. Rozanov[102], Z. M. A. Rozario[58], Y. Rozen[153], A. Rubio Jimenez[165], V.H. Ruelas Rivera[19], T.A. Ruggeri[1], A. Ruggiero[127], A. Ruiz-Martinez[165], A. Rummler[37], G.B. Rupnik Boero[37], N.A. Rusakovich[38], S. Ruscelli[48], H.L. Russell[167], G. Russo[137], J.P. Rutherfoord[7], S. Rutherford Colmenares[118], M. Rybar[134], P. Rybczynski[85a], A. Ryzhov[44], M. A. E. Saadawy[44], F. Safai Tehrani[74a], S. Saha[1], B. Sahoo[171], B. T. Saifuddin[121], M. Saimpert[136], I. Sainz Saenz Diez[62a], G.T. Saito[81c], M. Saito[156], T. Saito[156], A. Sala[70a,70b], O. T. Salin[65], A. Salnikov[146], J. Salt[165], A. Salvador Salas[154], F. Salvatore[149], A. Salzburger[37], D. Sammel[53], E. Sampson[91], D. Sampsonidis[155,ac], D. Sampsonidou[124], M.A.A. Samy[58], J. Sánchez[165], H. Sandaker[126], C.O. Sander[47], J.A. Sandesara[172], M. Sandhoff[173], C. Sandoval[23b], L. Sanfilippo[62a], D.P.C. Sankey[135], T. Sano[87], A. Sansar[22c], A. Sansoni[52], M. Santana Queiroz[18b], L. Santi[37], C. Santoni[40], G. Santoro[43b,43a], H. Santos[131a,131b], L. Santos Pereira Trigo[47], E. Sanzani[24b,24a], K.A. Saoucha[83d], J.G. Saraiva[131a,131d], J. Sardain[7], S. Sarkar[50], O. Sasaki[82], K. Sato[160], C. Sauer[37], E. Sauvan[4], P. Savard[158,t], M. Savic[164], R. Sawada[156], C. Sawyer[135], L. Sawyer[97], A. M. Sayed[27], C. Sbarra[24b], A. Sbrizzi[24b,24a], R. Scaglioni[72a,72b], T. Scanlon[96], J. Schaarschmidt[140], U. Schäfer[100], A.C. Schaffer[65,44], D. Schaile[109], R.D. Schamberger[148], C. Scharf[19], M.M. Schefer[20], D. Scheirich[134], M. Schernau[138f], C. Scheulen[55], C. Schiavi[56b,56a], M. Schioppa[43b,43a], S. Schlenker[37], T. Schlomer[54], J. Schmeing[173], C. R. Schmidt[49], E. Schmidt[110], M. A. Schmidt[173], K. Schmieden[25], C. Schmitt[100], N. Schmitt[100], S. Schmitt[47], N.A. Schneider[109], L. Schoeffel[136], A. Schoening[62b], P.G. Scholer[35], E. Schopf[144], M. Schott[25], S. Schramm[55], T. Schroer[55], H-C. Schultz-Coulon[62a], M. Schumacher[53], B.A. Schumm[137], Ph. Schune[136],

JHEP10(2026)206

H.R. Schwartz[7], A. Schwartzman[146], T.A. Schwarz[106], Ph. Schwemling[136], R. Schwienhorst[107], F.G. Sciacca[20], A. Sciandra[30], G. Sciolla[27], S. A. Scoville[130], F. Scuri[73a], C.D. Sebastiani[37], K. Sedlaczek[117], A. Sehrawat[138b], S.C. Seidel[114], B.D. Seidlitz[41], C. Seitz[47], J.M. Seixas[81b], G. Sekhniaidze[71a], L. Selem[128], N. Semprini-Cesari[24b,24a], A. Semushin[175], V. Senthilkumar[116], L. Serin[65], M. Sessa[71a,71b], H. Severini[121], F. Sforza[56b,56a], A. Sfyrla[55], Q. Sha[14], H. Shaddix[117], A.H. Shah[33], R. Shaheen[147], J.D. Shahinian[129], M. Shamim[37], L.Y. Shan[14], M. Shapiro[18a], A. Sharma[37], A.S. Sharma[166], P. Sharma[30], K. Shaw[149], S.M. Shaw[101], D. Shemyakin[171], Q. Shen[14], D.J. Sheppard[145], P. Sherwood[96], L. Shi[112b], X. Shi[14], E.B. Shields[171], S. Shimizu[82], S. Shirabe[88], M. Shiyakova[38,al], M.J. Shochet[39], D.R. Shope[126], S. Shrestha[120,am], I. Shreyber[38], M.J. Shroff[104], P. Sicho[132], A.M. Sickles[164], E. Sideras Haddad[34j], A. C. Sidley[116], A. Sidoti[24b], F. Siegert[49], Dj. Sijacki[16], F. Sili[61], J.M. Silva[51], I. Silva Ferreira[81b], M.V. Silva Oliveira[30], S.B. Silverstein[46a], S. Simion[65], R. Simoniello[37], E.L. Simpson[101], H. Simpson[149], L.R. Simpson[6], S. Simsek[80], S. Singh[30], S. N. Singh[27], S. Sinha[47], S. Sinha[101], M. Sioli[24b,24a], K. Sioulas[9], E. Sitnikova[47], J. Sjölin[46a,46b], A. Skaf[54], E. Skorda[21], P. Skubic[121], M. Slawinska[86], I. Slazyk[17], I. Sliusar[126], V. Smakhtin[171], B.H. Smart[135], S.Yu. Smirnov[138b], Y. Smirnov[34c], O. Smirnova[98], J.L. Smith[101], M. B. Smith[35], R. Smith[146], H. Smitmanns[100], M. Smizanska[91], K. Smolek[133], P. Smolyanskiy[133], A.A. Snesarev[38], H.L. Snoek[116], R. M. Snyder[50], S. Snyder[30], R. Sobie[167,o], A. Soffer[154], C.A. Solans Sanchez[37], E.Yu. Soldatov[38], U. Soldevila[165], A.A. Solodkov[34j], S. Solomon[27], A. Soloshenko[38], O.V. Solovyanov[40], P. Sommer[49], A. Sopczak[133], A.L. Sopio[51], F. Sopkova[29b], J. D. Sorenson[114], I.R. Sotarriva Alvarez[139], V. Sothilingam[62a], O. J. Soto Sandoval[138c,138b], S. Sottocornola[67], R. Soualah[83a], D. South[47], N. Soybelman[171], S. Spagnolo[69a,69b], A.S. Spellman[124], D. Sperlich[53], B. Spisso[71a,71b], L. Splendori[102], M. Spousta[134], E.J. Staats[35], R. Stamen[62a], E. Stanecka[86], W. Stanek-Maslouska[47], M.V. Stange[49], B. Stanislaus[18a], M.M. Stanitzki[47], G.H. Stark[137], J. Stark[89], P. Staroba[132], P. Starovoitov[83d], R. Staszewski[86], C. Stauch[109], G. Stavropoulos[45], A. Stefl[37], A. Stein[100], P. Steinberg[30], B. Stelzer[145,159a], H.J. Stelzer[130], O. Stelzer[159a], H. Stenzel[57], T.J. Stevenson[149], G.A. Stewart[47], G. Stoicea[28b], M. Stolarski[131a], S. Stonjek[110], A. Straessner[49], J. Strandberg[147], S. Strandberg[46a,46b], M. Stratmann[173], M. Strauss[121], T. Strebler[102], P. Strizenec[29b], R. Ströhmer[168], D.M. Strom[124], R. Stroynowski[44], A. Strubig[46a,46b], S.A. Stucci[30], B. Stugu[17], J. Stupak[121], N.A. Styles[47], D. Su[146], S. Su[61], X. Su[61], D. Suchy[29a], A. D. Sudhakar Ponnu[54], L. Sudit[171], Y. Sue[82], K. Sugizaki[129], D.M.S. Sultan[127], L. Sultanaliyeva[25], S. Sultansoy[3b], S. Sun[172], W. Sun[14], S. Sundar Raman[166], N. Sur[98], J.P. Surdutovich[120], N. Suri Jr[174], M.R. Sutton[149], M. Svatos[132], P. N. Swallow[33], S.N. Swatman[37], M. Swiatlowski[159a], A. Swoboda[37], I. Sykora[29a], M. Sykora[134], T. Sykora[134], D. Ta[100], K. Tackmann[47,an], A. Taffard[162], R. Tafirout[159a], Y. Takubo[82], M. Talby[102], N.M. Tamir[154], A. Tanaka[156], J. Tanaka[156], R. Tanaka[65], M. Tanasini[148], Z. Tao[166], S. Tapia Araya[138g], S. Tapprogge[100], A. Tarek Abouelfadl Mohamed[37], S. Tarem[153], K. Tariq[14], G. Tarna[37], G.F. Tartarelli[70a], M. J. Tartarin[141b], P. Tas[134], M. Tasevsky[132], E. Tassi[43b,43a], A.C. Tate[164], Y. Tayalati[36e,ao], G.N. Taylor[105],

JHEP10(2026)206

W. Taylor[159b], R.J. Taylor Vara[165], A.S. Tegetmeier[89], P. Teixeira-Dias[95], J.J. Teoh[158], K. Terashi[156], J. Terron[99], S. Terzo[13], M. Testa[52], R.J. Teuscher[158,o], A. Thaler[78], T. Theveneaux-Pelzer[102], J.P. Thomas[21], E.A. Thompson[18a], P.D. Thompson[21], E. Thomson[129], R. E. Thornberry[30], T.M. Thory-Rao[21], C.N. Thotamuna Wijewardhana[148], C. Tian[61], Y. Tian[55], V. Tikhomirov[80], Yu.A. Tikhonov[38], D. Timoshyn[134], E.X.L. Ting[1], P. Tipton[174], A. Tishelman-Charny[30], K. Todome[139], S. Todorova-Nova[134], L. Toffolin[68a,68c], M. Togawa[82], J. Tojo[88], S. Tokár[29a], O. Toldaiev[67], A. J. Toler[103], G. Tolkachev[102], M. Tomoto[82], L. Tompkins[146], E. Torrence[124], H. Torres[89], D. I. Torres Arza[138g], E. Torres Reoyo[165], E. Torró Pastor[165], M. Toscani[31], C. Tosciri[39], M. Tost[11], D.R. Tovey[142], T. Trefzger[168], P.M. Tricarico[13], A. Tricoli[30], I.M. Trigger[159a], S. Trincaz-Duvoid[128], D.A. Trischuk[167], A. Tropina[38], D. Truncali[75a,75b], L. Truong[34c], M. Trzebinski[86], A. Trzupek[86], F. Tsai[148], A. Tsiamis[155], P.V. Tsiareshka[38], S. Tsigaridas[159a], A. Tsirigotis[155,ad], V. Tsiskaridze[152a], E.G. Tskhadadze[152a], H. F. Tsoi[129], Y. Tsujikawa[87], V. Tsulaia[18a], K. Tsuri[119], D. Tsybychev[148], Y. Tu[63b], A. Tudorache[28b], V. Tudorache[28b], S. B. Tuncay[127], S. Turchikhin[56b,56a], I. Turk Cakir[3a], R. Turra[70a], T. Turtuvshin[38,ap], P.M. Tuts[41], Y. Uematsu[82], F. Ukegawa[160], P.A. Ulloa Poblete[138c,138b], G. Unal[37], A. Undrus[30], J. Urban[29b], P. Urrejola[138e], G. Usai[8], R. Ushioda[157], M. Usman[108], F. Ustuner[51], Z. Uysal[80], V. Vacek[133], B. Vachon[104], A. Vaitkus[96], C. Valderanis[109], E. Valdes Santurio[46a,46b], M. Valente[37], S. Valentinetti[24b,24a], A. Valero[165], E. Valiente Moreno[165], A. Vallier[89], J.A. Valls Ferrer[165], D. R. Van Arneman[116], R. Van Den Broucke[128], A. Van Der Graaf[48], H. Z. Van Der Schyf[34j], P. Van Gemmeren[6], M. Van Rijnbach[37], S. Van Stroud[96], I. Van Vulpen[116], P. Vana[134], M. Vanadia[75a,75b], U. M. Vande Voorde[147], W. Vandelli[37], E.R. Vandewall[146], D. Vannicola[154], R. Vari[74a], M. Varma[174], E.W. Varnes[7], C. Varni[85a], D. Varouchas[65], L. Varriale[165], K.E. Varvell[150], M.E. Vasile[28b], A. Vasileiadou[9], L. Vaslin[82], M. D. Vassilev[146], A. Vasyukov[38], L. M. Vaughan[122], R. Vavricka[134], T. Vazquez Schroeder[13], J. Veatch[32], V. Vecchio[101], M.J. Veen[103], I. Veliscek[30], I. Velkovska[93], L.M. Veloce[158], F. Veloso[131a,131c], A.G. Veltman[51], S.H. Venetianer[161], S. Veneziano[74a], A. Ventura[69a,69b], A. Verbytskyi[110], M. Verducci[73a,73b], C. Vergis[94], M. Verissimo De Araujo[81b], W. Verkerke[116], J.C. Vermeulen[116], C. Vernieri[146], M. Vessella[162], M.C. Vetterli[145,t], A. Vgenopoulos[100], N. Viaux Maira[138g,aq], L. Vicenik[133], T. Vickey[142], O.E. Vickey Boeriu[142], G.H.A. Viehhauser[127], L. Vigani[62b], M. Vigl[110], M. Villa[24b,24a], M. Villaplana Perez[165], E.M. Villhauer[39], E. Vilucchi[52], M. Vincent[165], M.G. Vincter[35], A. Visibile[116], A. Visive[116], C. Vittori[24b,24a], I. Vivarelli[24b,24a], M.I. Vivas Albornoz[47], E. Voevodina[110], F. Vogel[109], J.C. Voigt[136], P. Vokac[133], Yu. Volkotrub[85b], L. Vomberg[25], E. Von Toerne[25], B. Vormwald[37], K. Vorobev[50], M. Vos[165], K. Voss[144], M. Vozak[37], L. Vozdecky[121], N. Vranjes[16], M. Vranjes Milosavljevic[16], M. Vreeswijk[116], N.K. Vu[112a], R. Vuillermet[37], I. Vukotic[39], I. K. Vyas[35], J.F. Wack[33], A. Wada[111], S. Wada[160], C. Wagner[146], J.M. Wagner[18a], W. Wagner[173], S. Wahdan[173], H. Wahlberg[90], C. H. Waits[121], J. Walder[135], R. Walker[109], K. Walkingshaw Pass[58], W. Walkowiak[144], A. Wall[129], E.J. Wallin[98], T. Wamorkar[146], K. Wandall-Christensen[165], A. Wang[61], A.Z. Wang[137], C. Wang[47], C. Wang[11], H. Wang[18a], J. Wang[63c], P. Wang[101],

JHEP10(2026)206

P. Wang[96], R. Wang[60], R. Wang[106], R. Wang[6], S. Wang[14,ar], S.M. Wang[151], T. Wang[115], T. Wang[61], W. Wang[113c], W.T. Wang[127], X. Wang[164], X. Wang[141a], X. Wang[47], Y. Wang[148], Y. Wang[114], Z. Wang[14], Z. Wang[63b], C. Wanotayaroj[82], A. Warburton[104], A.L. Warnerbring[144], S. Waterhouse[96], A.T. Watson[21], H. Watson[51], M.F. Watson[21], E. Watton[37], G. Watts[140], B.M. Waugh[96], J. M. Webb[53], C. Weber[30], M.S. Weber[20], C. Wei[61], Y. Wei[53], A.R. Weidberg[127], E.J. Weik[118], J. Weingarten[48], C. Weiser[53], C.J. Wells[47], P.S. Wells[37], T. Wenaus[30], T. Wengler[37], N.S. Wenke[110], N. Wermes[25], D. Werner[47], M. Wessels[62a], A.M. Wharton[91], A. White[8], A.S. White[37], M.J. White[1], D. Whiteson[162], W. Wiedenmann[172], M. Wielers[135], R. Wierda[147], C. Wiglesworth[42], H.G. Wilkens[37], J. J. H. Wilkinson[33], S. Williams[33], S. Willocq[103], D.J. Wilson[101], P.J. Windischhofer[39], F.I. Winkel[31], F. Winklmeier[124], B.T. Winter[53], M. Wittgen[146], M. Wobisch[97], T. Wojtkowski[59], Z. Wolffs[116], J. Wollrath[37], M.W. Wolter[86], H. Wolters[131a,131c], M.C. Wong[137], E.L. Woodward[41], S.D. Worm[47], B.K. Wosiek[86], K. A. Wozniak[55], K.W. Woźniak[86], S. Wozniewski[54], K. Wraight[58], C. Wu[158], J. Wu[156], M. Wu[112b], M. Wu[115], S. Wu[14,ar], S.L. Wu[172], X. Wu[61], Y. Wu[61], Y.Q. Wu[158], Z. Wu[102], Z. Wu[112a], J. Wuerzinger[110], T.R. Wyatt[101], B.M. Wynne[51], S. Xella[42], L. Xia[112a], M. Xie[61], A. Xiong[124], I. Xiotidis[37], D. Xu[14], H. Xu[61], L. Xu[61], R. Xu[129], T. Xu[106], W. Xu[112a], Y. Xu[140], Z. Xu[51], R. Xue[130], B. Yabsley[150], S. Yacoob[11], Y. Yamaguchi[82], E. Yamashita[156], H. Yamauchi[160], T. Yamazaki[18a], Y. Yamazaki[84], F. Yan[2], S. Yan[58], Z. Yan[103], C. Yang[18a], H.J. Yang[141a], H.T. Yang[61], S. Yang[61], X. Yang[37], X. Yang[14], Y. Yang[156], Y. Yang[61], W-M. Yao[18a], C. L. Yardley[149], J. Ye[14], S. Ye[30], X. Ye[106], I. Yeletskikh[38], B. Yeo[18b], M.R. Yexley[96], T. P. Yildirim[127], K. Yorita[156], C. Young[146], C.J.S. Young[37], I.N.L. Young[58], N.D. Young[124], D. Yu[141b,5], Y. Yu[61], J. Yuan[14,112c,ar], M. Yuan[106], R. Yuan[141b], L. Yue[96], M. Zaazoua[61], B. Zabinski[86], I. Zahir[36a], Q.U.A. Zahoor[51], A. Zaio[56b,56a], Z.K. Zak[86], T. Zakareishvili[165], S. Zambito[55], J. Zang[156], R. Zanzottera[70a,70b], O. Zaplatilek[133], I. Zatocilova[53], E. Zaya[147], C. Zeitnitz[173], H. Zeng[14], T. Ženiš[29a], S. Zenz[94], W. Zhan[61], B. Zhang[169], D.F. Zhang[142], G. Zhang[14,ar], J. Zhang[113b], J. Zhang[6], L. Zhang[61], L. Zhang[112a], P. Zhang[14,112c], R. Zhang[112a], S. Zhang[14], Y. Zhang[140], Y. Zhang[96], Y. Zhang[61], Y. Zhang[112a], Z. Zhang[149], Z. Zhang[101], Z. Zhang[18a], Z. Zhang[113b], Z. Zhang[65], H. Zhao[140], T. Zhao[113b], Y. Zhao[35], Z. Zhao[61], Z. Zhao[61], A. Zhemchugov[38], J. Zheng[112a], K. Zheng[164], L. Zheng[113b], X. Zheng[61], Z. Zheng[146], D. Zhong[164], B. Zhou[106], B. Zhou[141b,141a], N. Zhou[141a], Y. Zhou[15], Y. Zhou[112a], Y. Zhou[7], Z. Zhou[61], J. Zhu[106], X. Zhu[141b], Y. Zhu[141a], X. Zhuang[14], K. Zhukov[67], P. Ziakas[4], N.I. Zimine[38], J. Zinsser[62b], M. Ziolkowski[144], L. Živković[16], A. Zoccoli[24b,24a], K. Zoch[37], A. Zografos[37], T.G. Zorbas[142], D. Zubov[155], L. Zwalinski[37]

[1] *Department of Physics, University of Adelaide, Adelaide, Australia*
[2] *Department of Physics, University of Alberta, Edmonton AB, Canada*
[3a] *Department of Physics, Ankara University, Ankara, Türkiye*
[3b] *Division of Physics, TOBB University of Economics and Technology, Ankara, Türkiye*
[4] *LAPP, Université Savoie Mont Blanc, CNRS/IN2P3, Annecy, France*
[5] *APC, Université Paris Cité, CNRS/IN2P3, Paris, France*
[6] *High Energy Physics Division, Argonne National Laboratory, Argonne IL, U.S.A.*
[7] *Department of Physics, University of Arizona, Tucson AZ, U.S.A.*

JHEP10(2026)206

[8] Department of Physics, University of Texas at Arlington, Arlington TX, U.S.A.
[9] Physics Department, National and Kapodistrian University of Athens, Athens, Greece
[10] Physics Department, National Technical University of Athens, Zografou, Greece
[11] Department of Physics, University of Texas at Austin, Austin TX, U.S.A.
[12] Institute of Physics, Azerbaijan Academy of Sciences, Baku, Azerbaijan
[13] Institut de Física d'Altes Energies (IFAE), Barcelona Institute of Science and Technology, Barcelona, Spain
[14] Institute of High Energy Physics, Chinese Academy of Sciences, Beijing, China
[15] Physics Department, Tsinghua University, Beijing, China
[16] Institute of Physics, University of Belgrade, Belgrade, Serbia
[17] Department for Physics and Technology, University of Bergen, Bergen, Norway
[18a] Physics Division, Lawrence Berkeley National Laboratory, Berkeley CA, U.S.A.
[18b] University of California, Berkeley CA, U.S.A.
[19] Institut für Physik, Humboldt Universität zu Berlin, Berlin, Germany
[20] Albert Einstein Center for Fundamental Physics and Laboratory for High Energy Physics, University of Bern, Bern, Switzerland
[21] School of Physics and Astronomy, University of Birmingham, Birmingham, U.K.
[22a] Department of Physics, Bogazici University, Istanbul, Türkiye
[22b] Department of Physics Engineering, Gaziantep University, Gaziantep, Türkiye
[22c] Department of Physics, Istanbul University, Istanbul, Türkiye
[23a] Facultad de Ciencias y Centro de Investigaciónes, Universidad Antonio Nariño, Bogotá, Colombia
[23b] Departamento de Física, Universidad Nacional de Colombia, Bogotá, Colombia
[24a] Dipartimento di Fisica e Astronomia A. Righi, Università di Bologna, Bologna, Italy
[24b] INFN Sezione di Bologna, Italy
[25] Physikalisches Institut, Universität Bonn, Bonn, Germany
[26] Department of Physics, Boston University, Boston MA, U.S.A.
[27] Department of Physics, Brandeis University, Waltham MA, U.S.A.
[28a] Transilvania University of Brasov, Brasov, Romania
[28b] Horia Hulubei National Institute of Physics and Nuclear Engineering, Bucharest, Romania
[28c] Department of Physics, Alexandru Ioan Cuza University of Iasi, Iasi, Romania
[28d] National Institute for Research and Development of Isotopic and Molecular Technologies, Physics Department, Cluj-Napoca, Romania
[28e] National University of Science and Technology Politechnica, Bucharest, Romania
[28f] West University in Timisoara, Timisoara, Romania
[28g] Faculty of Physics, University of Bucharest, Bucharest, Romania
[29a] Faculty of Mathematics, Physics and Informatics, Comenius University, Bratislava, Slovak Republic
[29b] Department of Subnuclear Physics, Institute of Experimental Physics of the Slovak Academy of Sciences, Kosice, Slovak Republic
[30] Physics Department, Brookhaven National Laboratory, Upton NY, U.S.A.
[31] Universidad de Buenos Aires, Facultad de Ciencias Exactas y Naturales, Departamento de Física, y CONICET, Instituto de Física de Buenos Aires (IFIBA), Buenos Aires, Argentina
[32] California State University, CA, U.S.A.
[33] Cavendish Laboratory, University of Cambridge, Cambridge, U.K.
[34a] Department of Physics, University of Cape Town, Cape Town, South Africa
[34b] iThemba Labs, Western Cape, South Africa
[34c] Department of Mechanical Engineering Science, University of Johannesburg, Johannesburg, South Africa
[34d] National Institute of Physics, University of the Philippines Diliman (Philippines), Philippines
[34e] Department of Physics, Stellenbosch University, Matieland, South Africa
[34f] University of KwaZulu-Natal, School of Agriculture and Science, Mathematics, Westville, South Africa
[34g] University of South Africa, Department of Physics, Pretoria, South Africa
[34h] University of Pretoria, Department of Mechanical and Aeronautical Engineering, Pretoria, South Africa
[34i] University of Zululand, KwaDlangezwa, South Africa
[34j] School of Physics, University of the Witwatersrand, Johannesburg, South Africa

JHEP10(2026)206

[35] Department of Physics, Carleton University, Ottawa ON, Canada
[36a] Faculté des Sciences Ain Chock, Université Hassan II de Casablanca, Morocco
[36b] Faculté des Sciences, Université Ibn-Tofail, Kénitra, Morocco
[36c] Faculté des Sciences Semlalia, Université Cadi Ayyad, LPHEA-Marrakech, Morocco
[36d] LPMR, Faculté des Sciences, Université Mohamed Premier, Oujda, Morocco
[36e] Faculté des sciences, Université Mohammed V, Rabat, Morocco
[36f] Institute of Applied Physics, Mohammed VI Polytechnic University, Ben Guerir, Morocco
[37] CERN, Geneva, Switzerland
[38] Affiliated with an international laboratory covered by a cooperation agreement with CERN
[39] Enrico Fermi Institute, University of Chicago, Chicago IL, U.S.A.
[40] LPC, Université Clermont Auvergne, CNRS/IN2P3, Clermont-Ferrand, France
[41] Nevis Laboratory, Columbia University, Irvington NY, U.S.A.
[42] Niels Bohr Institute, University of Copenhagen, Copenhagen, Denmark
[43a] Dipartimento di Fisica, Università della Calabria, Rende, Italy
[43b] INFN Gruppo Collegato di Cosenza, Laboratori Nazionali di Frascati, Italy
[44] Physics Department, Southern Methodist University, Dallas TX, U.S.A.
[45] National Centre for Scientific Research "Demokritos", Agia Paraskevi, Greece
[46a] Department of Physics, Stockholm University, Sweden
[46b] Oskar Klein Centre, Stockholm, Sweden
[47] Deutsches Elektronen-Synchrotron DESY, Hamburg and Zeuthen, Germany
[48] Fakultät Physik, Technische Universität Dortmund, Dortmund, Germany
[49] Institut für Kern- und Teilchenphysik, Technische Universität Dresden, Dresden, Germany
[50] Department of Physics, Duke University, Durham NC, U.S.A.
[51] SUPA – School of Physics and Astronomy, University of Edinburgh, Edinburgh, U.K.
[52] INFN e Laboratori Nazionali di Frascati, Frascati, Italy
[53] Physikalisches Institut, Albert-Ludwigs-Universität Freiburg, Freiburg, Germany
[54] II. Physikalisches Institut, Georg-August-Universität Göttingen, Göttingen, Germany
[55] Département de Physique Nucléaire et Corpusculaire, Université de Genève, Genève, Switzerland
[56a] Dipartimento di Fisica, Università di Genova, Genova, Italy
[56b] INFN Sezione di Genova, Italy
[57] II. Physikalisches Institut, Justus-Liebig-Universität Giessen, Giessen, Germany
[58] SUPA – School of Physics and Astronomy, University of Glasgow, Glasgow, U.K.
[59] LPSC, Université Grenoble Alpes, CNRS/IN2P3, Grenoble INP, Grenoble, France
[60] Laboratory for Particle Physics and Cosmology, Harvard University, Cambridge MA, U.S.A.
[61] Department of Modern Physics and State Key Laboratory of Particle Detection and Electronics, University of Science and Technology of China, Hefei, China
[62a] Kirchhoff-Institut für Physik, Ruprecht-Karls-Universität Heidelberg, Heidelberg, Germany
[62b] Physikalisches Institut, Ruprecht-Karls-Universität Heidelberg, Heidelberg, Germany
[63a] Department of Physics, Chinese University of Hong Kong, Shatin, N.T., Hong Kong, China
[63b] Department of Physics, University of Hong Kong, Hong Kong, China
[63c] Department of Physics and Institute for Advanced Study, Hong Kong University of Science and Technology, Clear Water Bay, Kowloon, Hong Kong, China
[64] Department of Physics, National Tsing Hua University, Hsinchu, Taiwan
[65] IJCLab, Université Paris-Saclay, CNRS/IN2P3, 91405, Orsay, France
[66] Centro Nacional de Microelectrónica (IMB-CNM-CSIC), Barcelona, Spain
[67] Department of Physics, Indiana University, Bloomington IN, U.S.A.
[68a] INFN Gruppo Collegato di Udine, Sezione di Trieste, Udine, Italy
[68b] ICTP, Trieste, Italy
[68c] Dipartimento Politecnico di Ingegneria e Architettura, Università di Udine, Udine, Italy
[69a] INFN Sezione di Lecce, Italy
[69b] Dipartimento di Matematica e Fisica, Università del Salento, Lecce, Italy
[70a] INFN Sezione di Milano, Italy
[70b] Dipartimento di Fisica, Università di Milano, Milano, Italy

JHEP10(2026)206

[71a] INFN Sezione di Napoli, Italy
[71b] Dipartimento di Fisica, Università di Napoli, Napoli, Italy
[72a] INFN Sezione di Pavia, Italy
[72b] Dipartimento di Fisica, Università di Pavia, Pavia, Italy
[73a] INFN Sezione di Pisa, Italy
[73b] Dipartimento di Fisica E. Fermi, Università di Pisa, Pisa, Italy
[74a] INFN Sezione di Roma, Italy
[74b] Dipartimento di Fisica, Sapienza Università di Roma, Roma, Italy
[75a] INFN Sezione di Roma Tor Vergata, Italy
[75b] Dipartimento di Fisica, Università di Roma Tor Vergata, Roma, Italy
[76a] INFN Sezione di Roma Tre, Italy
[76b] Dipartimento di Matematica e Fisica, Università Roma Tre, Roma, Italy
[77a] INFN-TIFPA, Italy
[77b] Università degli Studi di Trento, Trento, Italy
[78] Universität Innsbruck, Department of Astro and Particle Physics, Innsbruck, Austria
[79] Department of Physics and Astronomy, Iowa State University, Ames IA, U.S.A.
[80] Istinye University, Sariyer, Istanbul, Türkiye
[81a] Departamento de Engenharia Elétrica, Universidade Federal de Juiz de Fora (UFJF), Juiz de Fora, Brazil
[81b] Universidade Federal do Rio De Janeiro COPPE/EE/IF, Rio de Janeiro, Brazil
[81c] Instituto de Física, Universidade de São Paulo, São Paulo, Brazil
[81d] Rio de Janeiro State University, Rio de Janeiro, Brazil
[81e] Federal University of Bahia, Bahia, Brazil
[82] KEK, High Energy Accelerator Research Organization, Tsukuba, Japan
[83a] Khalifa University of Science and Technology, Abu Dhabi, United Arab Emirates
[83b] New York University Abu Dhabi, Abu Dhabi, United Arab Emirates
[83c] United Arab Emirates University, Al Ain, United Arab Emirates
[83d] University of Sharjah, Sharjah, United Arab Emirates
[84] Graduate School of Science, Kobe University, Kobe, Japan
[85a] AGH University of Krakow, Faculty of Physics and Applied Computer Science, Krakow, Poland
[85b] Marian Smoluchowski Institute of Physics, Jagiellonian University, Krakow, Poland
[86] Institute of Nuclear Physics Polish Academy of Sciences, Krakow, Poland
[87] Faculty of Science, Kyoto University, Kyoto, Japan
[88] Research Center for Advanced Particle Physics and Department of Physics, Kyushu University, Fukuoka, Japan
[89] L2IT, Université de Toulouse, CNRS/IN2P3, UPS, Toulouse, France
[90] Instituto de Física La Plata, Universidad Nacional de La Plata and CONICET, La Plata, Argentina
[91] Physics Department, Lancaster University, Lancaster, U.K.
[92] Oliver Lodge Laboratory, University of Liverpool, Liverpool, U.K.
[93] Department of Experimental Particle Physics, Jožef Stefan Institute and Department of Physics, University of Ljubljana, Ljubljana, Slovenia
[94] Department of Physics and Astronomy, Queen Mary University of London, London, U.K.
[95] Department of Physics, Royal Holloway University of London, Egham, U.K.
[96] Department of Physics and Astronomy, University College London, London, U.K.
[97] Louisiana Tech University, Ruston LA, U.S.A.
[98] Fysiska institutionen, Lunds universitet, Lund, Sweden
[99] Departamento de Física Teorica C-15 and CIAFF, Universidad Autónoma de Madrid, Madrid, Spain
[100] Institut für Physik, Universität Mainz, Mainz, Germany
[101] School of Physics and Astronomy, University of Manchester, Manchester, U.K.
[102] CPPM, Aix-Marseille Université, CNRS/IN2P3, Marseille, France
[103] Department of Physics, University of Massachusetts, Amherst MA, U.S.A.
[104] Department of Physics, McGill University, Montreal QC, Canada
[105] School of Physics, University of Melbourne, Victoria, Australia
[106] Department of Physics, University of Michigan, Ann Arbor MI, U.S.A.

JHEP10(2026)206

[107] Department of Physics and Astronomy, Michigan State University, East Lansing MI, U.S.A.
[108] Group of Particle Physics, University of Montreal, Montreal QC, Canada
[109] Fakultät für Physik, Ludwig-Maximilians-Universität München, München, Germany
[110] Max-Planck-Institut für Physik (Werner-Heisenberg-Institut), München, Germany
[111] Graduate School of Science and Kobayashi-Maskawa Institute, Nagoya University, Nagoya, Japan
[112a] Department of Physics, Nanjing University, Nanjing, China
[112b] School of Science, Shenzhen Campus of Sun Yat-sen University, China
[112c] University of Chinese Academy of Science (UCAS), Beijing, China
[113a] School of Physics, Nankai University, Tianjin, China
[113b] Institute of Frontier and Interdisciplinary Science and Key Laboratory of Particle Physics and Particle Irradiation (MOE), Shandong University, Qingdao, China
[113c] School of Physics, Zhengzhou University, China
[114] Department of Physics and Astronomy, University of New Mexico, Albuquerque NM, U.S.A.
[115] Institute for Mathematics, Astrophysics and Particle Physics, Radboud University/Nikhef, Nijmegen, Netherlands
[116] Nikhef National Institute for Subatomic Physics and University of Amsterdam, Amsterdam, Netherlands
[117] Department of Physics, Northern Illinois University, DeKalb IL, U.S.A.
[118] Department of Physics, New York University, New York NY, U.S.A.
[119] Ochanomizu University, Otsuka, Bunkyo-ku, Tokyo, Japan
[120] Ohio State University, Columbus OH, U.S.A.
[121] Homer L. Dodge Department of Physics and Astronomy, University of Oklahoma, Norman OK, U.S.A.
[122] Department of Physics, Oklahoma State University, Stillwater OK, U.S.A.
[123] Palacký University, Joint Laboratory of Optics, Olomouc, Czech Republic
[124] Institute for Fundamental Science, University of Oregon, Eugene, OR, U.S.A.
[125] Graduate School of Science, University of Osaka, Osaka, Japan
[126] Department of Physics, University of Oslo, Oslo, Norway
[127] Department of Physics, Oxford University, Oxford, U.K.
[128] LPNHE, Sorbonne Université, Université Paris Cité, CNRS/IN2P3, Paris, France
[129] Department of Physics, University of Pennsylvania, Philadelphia PA, U.S.A.
[130] Department of Physics and Astronomy, University of Pittsburgh, Pittsburgh PA, U.S.A.
[131a] Laboratório de Instrumentação e Física Experimental de Partículas – LIP, Lisboa, Portugal
[131b] Departamento de Física, Faculdade de Ciências, Universidade de Lisboa, Lisboa, Portugal
[131c] Departamento de Física, Universidade de Coimbra, Coimbra, Portugal
[131d] Centro de Física Nuclear da Universidade de Lisboa, Lisboa, Portugal
[131e] Departamento de Física, Escola de Ciências, Universidade do Minho, Braga, Portugal
[131f] Departamento de Física Teórica y del Cosmos, Universidad de Granada, Granada (Spain), Spain
[131g] Departamento de Física, Instituto Superior Técnico, Universidade de Lisboa, Lisboa, Portugal
[132] Institute of Physics of the Czech Academy of Sciences, Prague, Czech Republic
[133] Czech Technical University in Prague, Prague, Czech Republic
[134] Charles University, Faculty of Mathematics and Physics, Prague, Czech Republic
[135] Particle Physics Department, Rutherford Appleton Laboratory, Didcot, U.K.
[136] IRFU, CEA, Université Paris-Saclay, Gif-sur-Yvette, France
[137] Santa Cruz Institute for Particle Physics, University of California Santa Cruz, Santa Cruz CA, U.S.A.
[138a] Departamento de Física, Pontificia Universidad Católica de Chile, Santiago, Chile
[138b] Millennium Institute for Subatomic physics at high energy frontier (SAPHIR), Santiago, Chile
[138c] Instituto de Investigación Multidisciplinario en Ciencia y Tecnología, y Departamento de Física, Universidad de La Serena, Chile
[138d] Universidad Andres Bello, Department of Physics, Santiago, Chile
[138e] Universidad San Sebastian, Recoleta, Chile
[138f] Instituto de Alta Investigación, Universidad de Tarapacá, Arica, Chile
[138g] Departamento de Física, Universidad Técnica Federico Santa María, Valparaíso, Chile
[139] Department of Physics, Institute of Science, Tokyo, Japan
[140] Department of Physics, University of Washington, Seattle WA, U.S.A.

JHEP10(2026)206

[141a] State Key Laboratory of Dark Matter Physics, School of Physics and Astronomy, Shanghai Jiao Tong University, Key Laboratory for Particle Astrophysics and Cosmology (MOE), SKLPPC, Shanghai, China
[141b] State Key Laboratory of Dark Matter Physics, Tsung-Dao Lee Institute, Shanghai Jiao Tong University, Shanghai, China
[142] Department of Physics and Astronomy, University of Sheffield, Sheffield, U.K.
[143] Department of Physics, Shinshu University, Nagano, Japan
[144] Department Physik, Universität Siegen, Siegen, Germany
[145] Department of Physics, Simon Fraser University, Burnaby BC, Canada
[146] SLAC National Accelerator Laboratory, Stanford CA, U.S.A.
[147] Department of Physics, Royal Institute of Technology, Stockholm, Sweden
[148] Departments of Physics and Astronomy, Stony Brook University, Stony Brook NY, U.S.A.
[149] Department of Physics and Astronomy, University of Sussex, Brighton, U.K.
[150] School of Physics, University of Sydney, Sydney, Australia
[151] Institute of Physics, Academia Sinica, Taipei, Taiwan
[152a] E. Andronikashvili Institute of Physics, Iv. Javakhishvili Tbilisi State University, Tbilisi, Georgia
[152b] High Energy Physics Institute, Tbilisi State University, Tbilisi, Georgia
[152c] University of Georgia, Tbilisi, Georgia
[153] Department of Physics, Technion, Israel Institute of Technology, Haifa, Israel
[154] Raymond and Beverly Sackler School of Physics and Astronomy, Tel Aviv University, Tel Aviv, Israel
[155] Department of Physics, Aristotle University of Thessaloniki, Thessaloniki, Greece
[156] International Center for Elementary Particle Physics and Department of Physics, University of Tokyo, Tokyo, Japan
[157] Graduate School of Science and Technology, Tokyo Metropolitan University, Tokyo, Japan
[158] Department of Physics, University of Toronto, Toronto ON, Canada
[159a] TRIUMF, Vancouver BC, Canada
[159b] Department of Physics and Astronomy, York University, Toronto ON, Canada
[160] Division of Physics and Tomonaga Center for the History of the Universe, Faculty of Pure and Applied Sciences, University of Tsukuba, Tsukuba, Japan
[161] Department of Physics and Astronomy, Tufts University, Medford MA, U.S.A.
[162] Department of Physics and Astronomy, University of California Irvine, Irvine CA, U.S.A.
[163] Department of Physics and Astronomy, University of Uppsala, Uppsala, Sweden
[164] Department of Physics, University of Illinois, Urbana IL, U.S.A.
[165] Instituto de Física Corpuscular (IFIC), Centro Mixto Universidad de Valencia – CSIC, Valencia, Spain
[166] Department of Physics, University of British Columbia, Vancouver BC, Canada
[167] Department of Physics and Astronomy, University of Victoria, Victoria BC, Canada
[168] Fakultät für Physik und Astronomie, Julius-Maximilians-Universität Würzburg, Würzburg, Germany
[169] Department of Physics, University of Warwick, Coventry, U.K.
[170] Waseda University, Tokyo, Japan
[171] Department of Particle Physics and Astrophysics, Weizmann Institute of Science, Rehovot, Israel
[172] Department of Physics, University of Wisconsin, Madison WI, U.S.A.
[173] Fakultät für Mathematik und Naturwissenschaften, Fachgruppe Physik, Bergische Universität Wuppertal, Wuppertal, Germany
[174] Department of Physics, Yale University, New Haven CT, U.S.A.
[175] Yerevan Physics Institute, Yerevan, Armenia

[a] Also at Department of Physics, King's College London, London, U.K.
[b] Also at Institute of Physics, Azerbaijan Academy of Sciences, Baku, Azerbaijan
[c] Also at Imam Mohammad Ibn Saud Islamic University, Saudi Arabia
[d] Also at Department of Physics, University of Thessaly, Greece
[e] Also at Département de Physique Nucléaire et Corpusculaire, Université de Genève, Genève, Switzerland
[f] Also at An-Najah National University, Nablus, Palestine
[g] Also at Department of Physics, University of Fribourg, Fribourg, Switzerland
[h] Also at Department of Physics, Westmont College, Santa Barbara, U.S.A.

JHEP10(2026)206

[i] Also at Departament de Fisica de la Universitat Autonoma de Barcelona, Barcelona, Spain
[j] Also at University of Siena, Italy
[k] Also at Affiliated with an institute formerly covered by a cooperation agreement with CERN
[l] Also at The Collaborative Innovation Center of Quantum Matter (CICQM), Beijing, China
[m] Also at Faculty of Physics, Sofia University, 'St. Kliment Ohridski', Sofia, Bulgaria
[n] Also at Università di Napoli Parthenope, Napoli, Italy
[o] Also at Institute of Particle Physics (IPP), Canada
[p] Also at Department of Physics, Bolu Abant Izzet Baysal University, Bolu, Türkiye
[q] Also at Faculty of Physics, University of Bucharest, Romania
[r] Also at Borough of Manhattan Community College, City University of New York, New York NY, U.S.A.
[s] Also at National Institute of Physics, University of the Philippines Diliman (Philippines), Philippines
[t] Also at TRIUMF, Vancouver BC, Canada
[u] Also at Universita degli Studi Link, Italy
[v] Also at Department of Financial and Management Engineering, University of the Aegean, Chios, Greece
[w] Also at University and INFN Torino, Torino, Italy
[x] Also at Institucio Catalana de Recerca i Estudis Avancats, ICREA, Barcelona, Spain
[y] Also at Henan University, China
[z] Also at Yeditepe University, Physics Department, Istanbul, Türkiye
[aa] Also at Institute of Theoretical Physics, Ilia State University, Tbilisi, Georgia
[ab] Also at CERN, Geneva, Switzerland
[ac] Also at Center for Interdisciplinary Research and Innovation (CIRI-AUTH), Thessaloniki, Greece
[ad] Also at Hellenic Open University, Patras, Greece
[ae] Also at Department of Modern Physics and State Key Laboratory of Particle Detection and Electronics, University of Science and Technology of China, Hefei, China
[af] Also at Department of Physics, Stellenbosch University, South Africa
[ag] Also at School of Physics, University of the Witwatersrand, Johannesburg, South Africa
[ah] Also at Department of Physics, Ben Gurion University of the Negev, Beer Sheva, Israel
[ai] Also at University of Colorado Boulder, Department of Physics, Colorado, U.S.A.
[aj] Also at Centre of Physics of the Universities of Minho and Porto (CF-UM-UP), Portugal
[ak] Also at Indian Institute of Technology (IIT), Jodhpur, India
[al] Also at Institute for Nuclear Research and Nuclear Energy (INRNE) of the Bulgarian Academy of Sciences, Sofia, Bulgaria
[am] Also at Washington College, Chestertown, MD, U.S.A.
[an] Also at Institut für Experimentalphysik, Universität Hamburg, Hamburg, Germany
[ao] Also at Institute of Applied Physics, Mohammed VI Polytechnic University, Ben Guerir, Morocco
[ap] Also at Institute of Physics and Technology, Mongolian Academy of Sciences, Ulaanbaatar, Mongolia
[aq] Also at Millennium Institute for Subatomic physics at high energy frontier (SAPHIR), Santiago, Chile
[ar] Also at University of Chinese Academy of Sciences (UCAS), Beijing, China
[†] Deceased

JHEP10(2026)206